American Journal of Pathology, Vol. 145, No. 6, December 1994

Synaptic Pathology and Glial Responses to Neuronal Injury Precede the Formation of Senile Plaques and Amyloid Deposits in the Aging Cerebral Cortex

Lee J. Martin,*‡‖ Carlos A. Pardo,*‖
Linda C. Cork,*§‖ and Donald L. Price*†‡‖

From the Departments of Pathology, Neurology,† and Neuroscience,‡ the Division of Comparative Medicine,§ and the Neuropathology Laboratory,‖ The Johns Hopkins University School of Medicine, Baltimore, Maryland*

The cerebral cortices of macaques (ranging in age from 10 to 37 years; n = 17) were analyzed by immunocytochemistry and electron microscopy to determine the cellular and subcellular localizations of the amyloid precursor protein and β-amyloid protein, the cellular participants in the formation of senile plaques and parenchymal deposits of the β-amyloid protein, and the temporal/spatial development of these lesions. Amyloid precursor protein was enriched within the cytoplasm of pyramidal and nonpyramidal neuronal cell bodies in young and old monkeys. In the neuropil, amyloid precursor protein was most abundant within dendrites and dendritic spines; few axons, axonal terminals, and resting astrocytes and microglia contained the amyloid precursor protein. At synapses, amyloid precursor protein was found predominantly within postsynaptic elements and was enriched at postsynaptic densities of asymmetrical synapses. The earliest morphological change related to senile plaque formation was an age-related abnormality in the cortical neuropil characterized by the formation of dense bodies within presynaptic terminals and dendrites and an augmented localization of the amyloid precursor protein to astrocytes and microglia. In most monkeys >26 years of age, the neocortical parenchyma exhibited neuritic pathology and plaques characterized by swollen cytoplasmic processes, interspersed somata of neurons, and reactive glia within or at the periphery of senile plaques. Neurites and reactive astrocytes and microglia within these plaques were enriched with the amyloid precursor protein. In diffuse plaques, nonfibrillar β-amyloid protein immunoreactivity was visualized within cytoplasmic lysosomes of neuronal perikarya and dendrites and the cell bodies and processes of activated astrocytes and microglia. In mature plaques, β-amyloid protein immunoreactivity was associated with extracellular fibrils within the parenchyma; some cytoplasmic membranes of degenerating dendrites and somata as well as processes of activated glia showed diffuse intracellular β-amyloid protein immunoreactivity. We conclude that morphological abnormalities at synapses (including changes in both pre- and postsynaptic elements) precede the accumulation of the amyloid precursor protein within neurites and activated astrocytes and microglia as well as the deposition of extracellular fibrillar β-amyloid protein; neuronal perikarya/dendrites and reactive glia containing the amyloid precursor protein are primary sources of the β-amyloid protein within senile plaques; and nonfibrillar β-amyloid protein exists intracellularly within neurons and nonneuronal cells prior to the appearance of extracellular deposits of the β-amyloid protein and the forma-

Supported by grants from the U.S. Public Health Service (NIH NS 07179, NS 20471, AG 05146, AG 05539). Dr. Pardo was supported by a Fellowship from the Fogarty Foundation. Dr. Price is the recipient of a Javits Neuroscience Investigator Award (NIH NS 10580). Drs. Price and Martin are the recipients of a Leadership and Excellence in Alzheimer's Disease (LEAD) award (NIA AG 07914).

Accepted for publication August 15, 1994.

This article is dedicated to the memory of Mr. Wayne Voris.

Linda C. Cork's current address is Stanford University School of Medicine, Stanford, California.

Address reprint requests to Lee J. Martin, Ph.D., The Johns Hopkins University School of Medicine, Neuropathology Laboratory, 720 Rutland Ave., 558 Ross Research Building, Baltimore, MD 21205–2196.

tion of β-pleated fibrils. We hypothesize that age-related perturbations in cell-cell interactions at synapses and subsequent synaptic degeneration and activation of astrocytes and microglia are early events that contribute to the formation of senile plaques and β-amyloid protein deposits within the cerebral cortex. (Am J Pathol 1994, 145:1358–1381)

Senile plaques are lesions that occur abundantly in the cerebral cortices of individuals with Alzheimer's disease (AD), patients with Down's syndrome, and, less frequently, in normal aged humans.[1–10] These lesions are heterogeneous and complex, consisting of dystrophic neurites, activated astrocytes and microglia, and extracellular deposits of amyloid fibrils.[4,7–10] Fibrils are composed of a 4-kd peptide (β-amyloid protein (Aβ))[11–13] consisting of 42 or 43 amino acid residues.[14] Aβ is derived proteolytically from amyloid precursor protein (APP), a cell-surface protein with a large N-terminal extracellular domain that contains 22 residues of Aβ, a hydrophobic membrane-spanning region including the transmembrane portion of the Aβ region, and a short C-terminal cytoplasmic segment.[15–17] The APP gene, located on human chromosome 21,[18–20] is spliced alternatively to form at least five different forms of APP transcripts and isoforms.[15,20] In cultured cells, APP normally undergoes constitutive proteolytic cleavage[17,21] by α-APP secretase, an enzyme that cleaves APP within the Aβ region,[22–25] thereby generating secreted forms of APP and preventing the formation of full-length Aβ derivatives.[22,23] Alternatively, APP may be processed by an endosomal-lysosomal pathway that, unlike the α-secretase pathway, yields amyloidogenic fragments of Aβ[26,27]; Aβ can be formed normally *in vivo* and *in vitro*.[28–30] An etiological role of APP in the pathogenesis of AD is supported further by the identification of mutations in the APP gene linked to early-onset AD in some families.[31–33]

The biological functions of APP are unknown, although APP may function at synapses.[34] Furthermore, the *in vivo* mechanisms responsible for Aβ deposition are still uncertain, as are the cellular sources of APP and Aβ. Neurons and possibly glial and vascular cells may represent different sources of APP and Aβ. Within senile plaques, the presence of abnormal neuronal processes, reactive cells, including astrocytes and microglia, and vascular elements suggests that a variety of cellular populations may serve as sources for the APP converted to Aβ.[35–40] However, the precise origins and temporal formations of plaques and Aβ deposits that occur within the neuropil of cerebral cortex are still uncertain. Analysis of the cellular localization of APP and the temporal development of senile plaques and Aβ deposits would provide needed insight into the origin of these lesions in cerebral cortex. Because aged nonhuman primates spontaneously develop dystrophic neurites, Aβ deposits, and plaques within the cerebral cortex,[10,39–43] these animals provide an excellent model for analyzing the evolution of these lesions and the cellular processes associated with these abnormalities. The present immunocytochemical (ICC) and electron microscopic (EM) studies of the cerebral cortex of monkeys were undertaken to determine the subcellular localizations of APP and Aβ and the cellular participants and early temporal structural alterations that eventuate in the formation of senile plaques and parenchymal deposits of Aβ in the cerebral cortex.

Materials and Methods

Male and female macaques ($n = 17$), ranging from 10 to 37 years of age, were used in this study (Table 1). Some brains were removed rapidly, blocked coronally, and frozen under dry ice. Sections of unfixed frozen brain were cut (10 μ) serially on a cryostat. For EM, monkeys were deeply anesthetized and perfused intracardially with normal saline, followed by varying concentrations of paraformaldehyde plus glutaraldehyde prepared in 0.1 mol/L phosphate buffer (pH 7.4) (Table 1). Fixed brains were removed

Table 1. *Nonhuman Primates From Which Brain Samples Were Obtained*

Type of Macaque	Age (years)*	Tissue Preparation†
Rhesus	31	4% PF (perfused)
Rhesus	26	4% PF (perfused)
Lion-tailed	>36	FF/4% PF (immersion)
Rhesus	15	FF/4% PF (immersion)
Rhesus	29	3% PF + 1% glut. (perfused)
Rhesus	N/A	4% PF (perfused)
Rhesus	N/A	3% PF + 0.2% glut. (perfused)
Cynomolgus	10	4% PF (perfused)
Rhesus	23	4% PF (perfused)
Cynomolgus	N/A	3% PF (perfused)
Rhesus	25	4% PF (perfused)
Cynomolgus	10	3.5% PF (perfused)
Rhesus	16	4% PF + 1% glut. (perfused)
Rhesus	27	4% PF + 1% glut. (perfused)
Pigtail	27	4% PF + 2% glut. (perfused)
Pigtail	28	4% PF + 2% glut. (perfused)
Lion-tailed	30	4% + 0.1% glut. (perfused)

* The precise ages of some monkeys were unknown and are indicated as N/A (not available).

† Abbreviations: PF, paraformaldehyde; FF, fresh-frozen; glut., glutaraldehyde.

and blocked coronally; samples were taken from dorsolateral and orbital frontal, anterior cingulate, superior and inferior temporal, occipital, and entorhinal cortices and hippocampus. Some samples (3 mm^3) for EM were osmicated immediately and embedded in plastic. Thin coronal slabs of cortex were postfixed (1 hour) in aldehydes, rinsed in several changes of phosphate-buffered saline (PBS), and cut (40 μ) on a Vibratome (Ted Pella, Inc., Redding, CA). Some sections of cerebral cortex were used for the histochemical visualization of cytochrome oxidase activity[44] and nicotinamide dinucleotide phosphate-diaphorase (NADPH).[45] Following NADPH-diaphorase histochemistry, selected sections were processed for ICC. All sections were pretreated with methanol/H_2O_2 to eliminate endogenous peroxidase activity and rinsed (30 minutes) in PBS. Sections intended for Aβ ICC were pretreated with formic acid or 1% sodium borohydride. Cryostat sections were treated with 0.4% Triton X-100; Vibratome sections were either permeabilized slightly (20 minutes), using 0.08% Triton X-100/PBS, or not exposed to detergent. Sections were blocked in 5% dry milk or 4% normal goat serum and incubated (48 hours) in one of the following antibodies (Table 2): a mouse monoclonal antibody (22C11) that recognizes an epitope located between amino acids 60 and 100 in the N-terminal region of the ectodomain of human APP[17]; a rabbit polyclonal antibody (Bx6) directed against the C-terminal region of APP[46]; rabbit polyclonal antipeptide antibody (CT15) raised against the terminal 15 amino acids of APP[25]; rabbit polyclonal antibodies that recognize amino acids 1–28 of the Aβ region[12]; mouse monoclonal antibodies (α-CD68 and HLA-DR), which are selective markers for cells derived from monocytes/macrophages (Dako, Carpinteria, CA); or mouse monoclonal and rabbit polyclonal antibodies that detect glial fibrillary acidic protein (GFAP). Using monkey brain, the specificities of anti-APP antibodies were characterized by immunoblotting and by preadsorption of anti-APP antibodies against denatured APP-695 synthesized in APP-695-transfected COS-1 cells prior to ICC staining.[40] The specificity of the Aβ immunoreactivity in sections of brain was evaluated by preadsorption of anti-Aβ antibody against synthetic $A\beta^{1-28}$ (Bachem, Torrance, CA) and APP. For additional controls, sections incubated with mouse immunoglobulin served as negative controls for sections incubated with monoclonal antibodies; sections incubated with normal rabbit serum served as negative controls for sections incubated with rabbit polyclonal antibodies. After incubation in primary antibody, sections were incubated sequentially with appropriate secondary antibodies (Cappel, West Chester, PA) and peroxidase-antiperoxidase complex (Sternberger Monoclonals, Baltimore, MD). A standard diaminobenzidine reaction was used to visualize immunoreactivities. After the disclosing reaction, some thick (40-μ) sections were mounted on slides for light microscopy; other sections were temporarily mounted on slides and viewed microscopically, and areas of cerebral cortex containing plaques or Aβ deposits were sampled for EM. All samples obtained from ICC-processed Vibratome sections were postfixed (1 hour) in 2% osmium tetroxide, dehydrated, stained *en bloc* with uranyl acetate, and flat embedded in resin. Plastic-embedded samples of Vibratome sections were mounted in an Epon block (Electron Microscopy Sciences, Fort Washington, PA) and cut into semithin (1-μ) and ultrathin sections for light microscopy and EM, respectively. All semithin sections were counterstained with toluidine blue before photography. Ultrathin sections, with and without lead citrate staining, were viewed with a Hitachi 600, Philips CM12, or JOEL 100S electron microscope. Ultrastructural criteria for the determination of cell type included the nuclear morphology, presence or absence of synaptic contacts, abundance and distribution of cytoplasmic organelles, and cytoskeletal features. Moreover, cells and processes were analyzed in serial ultrathin sections of the same sample.

Some sections were used to visualize two different antigens within the same tissue section.[47,48] Double immunolabeling was used to colocalize APP/GFAP, APP/CD68, Aβ/GFAP, and Aβ/CD68 using combinations of primary antibodies that were raised in different species. Briefly, the peroxidase-antiperoxidase method was used to detect the first antigen with diaminobenzidene as chromogen. The first-cycle antibodies were eluted (2 hours) with 0.2 mol/L glycine-HCl buffer (pH 2.2). Following successful elution of the first-cycle antibodies, the second antigen was detected with avidin-biotin kits with benzidine dihydrochloride as chromogen and 10 mM sodium acetate buffer (pH 6.0). Negative controls for dual labeling

Table 2. *Sources and Concentrations of Primary Antibodies Used in ICC Studies of Monkey Brain*

Antibody	Concentration	Source
α-APP (22C11)	1:500	K. Beyreuther
α-APP (Bx6)	1:500	T. Oltersdorf
α-APP (CT15)	1:2000	E. Koo
α-Aβ	1:750	C. Masters
α-CD68	1:100	Dako
α-HLA-DR	1:100	Dako
α-GFAP	1:1000–1:2000	Dako Boehringer Mannheim

ICC included omission of first- or second-cycle primary antibody and substitution of primary antibodies with normal serum.

Results

In frontal, cingulate, temporal, entorhinal, and occipital cortices and hippocampi of young and old monkeys, neuronal cell bodies and dendrites showed APP immunoreactivity (Figure 1). Different fixation strategies did not have a major effect on antigen localization. No species or age-related differences were apparent in the distributions of APP-immunoreactive neurons within these cortical regions. APP-immunoreactive neuronal cell bodies were visualized by antibodies that recognize N- and C-terminal domains of APP; preadsorption of antibodies against denatured APP (synthesized in APP-695 transfected COS-1 cells[23]) abolished immunoreactivity (Figure 1B). Only a subset (40 to 50%) of pyramidal neurons in layers III and V exhibited intense APP immunoreactivity (Figure 1A) as visualized by an N-terminal-specific monoclonal antibody (22C11), whereas the majority (>90%) of these neurons showed APP immunoreactivity as demonstrated by C-terminal-specific polyclonal antibodies (BX6 and CT15). Smaller intensely immunoreactive nonpyramidal neurons were localized in all layers. In hippocampus, APP immunoreactivity was localized to pyramidal neurons in CA1-CA4 and subiculum (Figure 1, D–F). Neocortical and hippocampal neurons exhibited variations in the intensities of APP immunoreactivity. Some neurons were devoid of APP immunoreactivity (Figure 1D), whereas other cells showed a high expression of APP (Figure 1, C and F). Some neuronal perikarya showed granular immunoreactivity that appeared to be located within the cytoplasm or associated with the

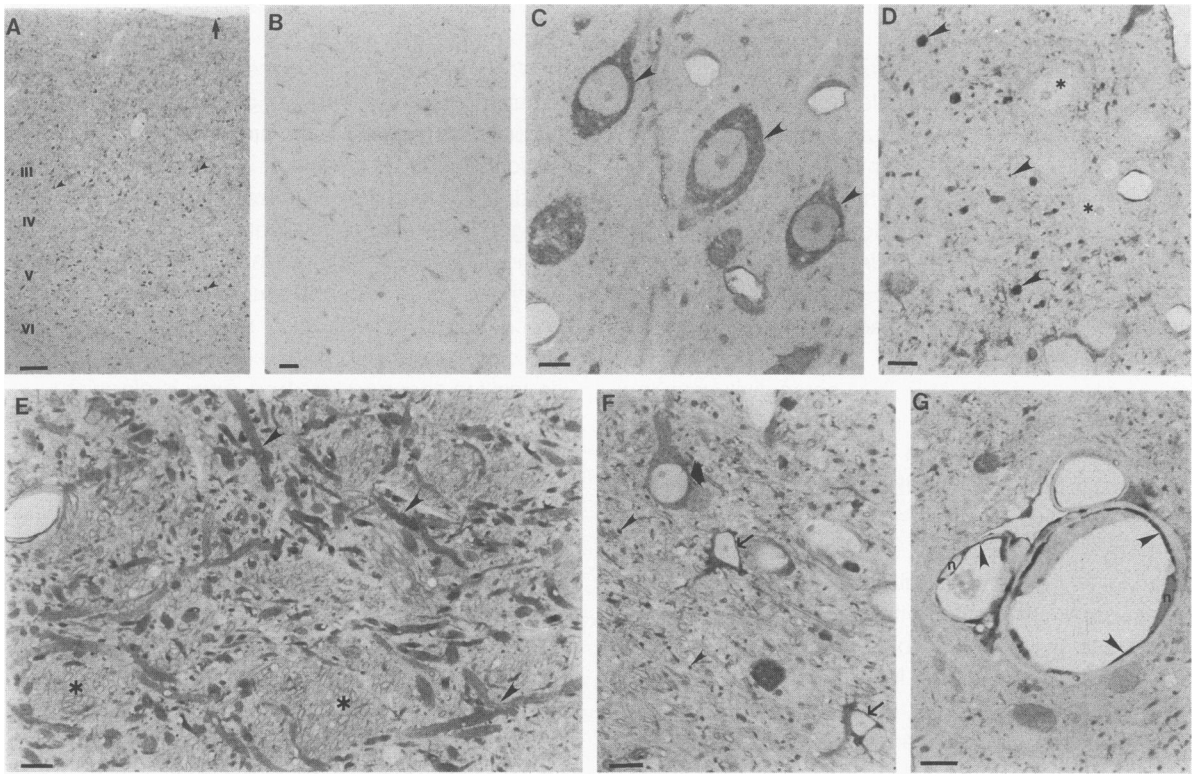

Figure 1. *Localization of APP in thick sections* (**A, B**) *and toluidine blue counterstained semithin* (*1 μ*) *plastic sections* (**C–G**) *of cerebral cortex from monkeys 10–26 years of age.* (**A**) *In frontal cortex of monkey 26 years of age* (*as well as other neocortical regions*), *APP-immunoreactive neurons* (*arrowheads*) *are distributed throughout all laminae but are most abundant in layers III and V. Arrow identifies the pial surface. Scale bar: 75 μ.* (**B**) *In control sections, immunoreactivity is abolished when anti-APP antibodies are incubated with denatured APP* (*synthesized in APP-695 transfected COS-1 cells*) *prior to use in ICC. Scale bar: 100 μ.* (**C**) *Some neuronal cell bodies* (*arrowheads*) *in entorbinal cortex express abundant APP immunoreactivity within the cytoplasm, whereas nuclei show no labeling. Scale bar = 7 μ.* (**D**) *The neuropil within CA4 of hippocampus contains ovoid and punctate APP-immunoreactive profiles* (*arrowheads*), *whereas nearby neuronal perikarya* (*asterisks*) *are not immunoreactive. Scale bar: 6.25 μ.* (**E**) *In hippocampus, many proximal dendritic shafts* (*arrowheads*), *seen in transverse and longitudinal profile, are enriched in APP immunoreactivity, but adjacent fascicles of axons* (*asterisks*) *are not immunoreactive. Scale bar: 7 μ.* (**F**) *In hippocampus, cell bodies and processes of astrocytes* (*thin arrows*) *as well as neurons* (*broad arrow*) *are APP immunoreactive. Small, round, APP-immunoreactive profiles* (*arrowheads*) *are also present in the neuropil. Scale bar: 6.5 μ.* (**G**) *Endothelial cells of blood vessels* (*arrowheads*) *in cerebral cortex express APP immunoreactivity. The nuclei of two endothelial cells* (*n*) *are in the plane of section. Scale bar: 8.13 μ.*

surface of the cell. Proximal dendrites were also immunopositive for APP (Figure 1, E and F).

In 1-μ plastic sections, punctate, oval, and linear APP-immunoreactive profiles were visualized in the neuropil; APP immunoreactivity was present within the cytoplasm of cell bodies and dendrites (Figure 1, C–E). Patterns of cellular immunoreactivity visualized with N- and C-terminal anti-APP antibodies were qualitatively similar. Immunostaining for APP was localized as discrete perinuclear granules within neuronal perikarya. In young and aged monkeys, qualitative differences in the intensity of immunostaining and distributions of neuronal APP immunoreactivity were not observed using light microscopy. However, in cerebral cortex from some aged monkeys (>26 years old), immunoreactivity for the C-terminal region of APP was associated with some large axons, similar to our observations using antibodies to the N-terminal region of APP.[40]

Within neocortex and hippocampus, APP immunoreactivity was also demonstrable within nonneuronal cells, including some astrocytes (Figure 1F), microglia (see Figure 8A), pericytes, and vascular endothelial cells (Figure 1G). Double-labeling ICC showed that APP and GFAP (see Figure 9A) as well as APP and CD68 (see Figure 8, A and C) colocalized, thus demonstrating the localization of APP to astrocytes and microglia, respectively. Reactive astrocytes and microglia in aged monkey brain were more frequently APP immunoreactive and were more enriched in APP (ie, more intensely immunoreactive) than resting glial cells (see Figure 8, A and C).

EM confirmed that APP immunoreactivity was localized within a subset of neuronal cell bodies and dendrites (Figure 2, A and C) as well as within nonneural cells (Figure 2, E and F) in monkeys of all ages. Immunoreactive perikarya and processes were identified by the amorphous, electron-dense immunoproduct formed by the diaminobenzidine reaction and subsequent staining with osmium tetroxide. Control sections were devoid of immunoreactivity. Electron-dense structures found in sections reacted with anti-APP antibodies, normal rabbit serum, or mouse immunoglobulin were interpreted as nonspecific labeling and attributed to the inherent osmophilia of some organelles (Figure 2B) and nonneuronal cells. APP immunoreactivity within perikarya and dendrites was distributed throughout the cytoplasm and on the surfaces of membranes of neuronal subsets. APP immunoreactivity appeared to be associated with the plasmalemma, Golgi membranes, and outer membranes of mitochondria (Figure 2D). Lysosomes and lipofuscin granules did not show definitive APP immunoreactivity. By EM, these structures were electron dense in both experimental and control sections (Figure 2B) from young and aged monkeys, and evaluation of these preparations at high magnification (30,000–40,000×) revealed no evidence of APP immunoreaction product associated with lysosomes and the vacuolar and granule components of lipofuscin granules. Neuronal cell bodies and dendrites enriched in APP immunoreactivity were in synaptic contact with numerous unlabeled presynaptic elements forming asymmetric synapses. APP immunoreactivity was often associated with the density of postsynaptic elements contacted by axodendritic asymmetric synapses (Figure 2C), which have an electron dense thickening of the junctional surface of the postsynaptic element (Figure 2, C and D). APP-immunoreactive structures in the neuropil observed in 1-μ-thick plastic sections (Figure 1D) were, by EM, predominantly cross sections of dendritic profiles (Figure 2, C and D) or glial cell processes (Figure 2E), but some APP-immunoreactive axons (Figure 2F), presynaptic elements, and capillary endothelial cells (Figure 2F) were also encountered in the neuropil.

Within the cerebral cortices of older monkeys (five of seven, >26 years of age), plaques were observed frequently (Figure 3), but neurofibrillary tangles were not found in any of these animals. Senile plaques and Aβ deposits were not visualized in animals <26 years of age. The presence of plaques and deposits of Aβ within different areas of cerebral cortex was variable, but these lesions occurred most frequently in dorsolateral frontal, orbitofrontal, and superior temporal cortices. In old monkeys, senile plaques and Aβ deposition occurred less frequently in cingulate, entorhinal, inferior temporal, and occipital cortices and rarely in hippocampus. Most plaques in aged macaques were diffuse or primitive with no amyloid cores; plaques with amyloid cores occurred infrequently in aged monkeys. In most primitive and in some advanced diffuse plaques, extracellular amyloid fibrils (8 to 10 nm) and fibrillar Aβ immunoreactivity were observed. In early diffuse plaques (defined ultrastructurally as focal structural abnormalities of the neuropil as evidenced by loss of synaptic integrity and pre- and postsynaptic inclusions or dense bodies) (Figure 4), Aβ immunoreactivity or 8 to 10-nm amyloid fibrils were not observed.

Low-magnification EM of cerebral cortex illustrates the heterogeneous composition and complexity of a primitive plaque (Figure 3). Mature neuritic plaques were characterized by a highly disrupted neuropil that contained large, swollen cytoplasmic processes, interspersed cells (neuronal, astrocytic, and microglial), and extracellular deposits of amyloid fibrils (8 to 10 nm). Swollen neurites were spherical, ovoid, or

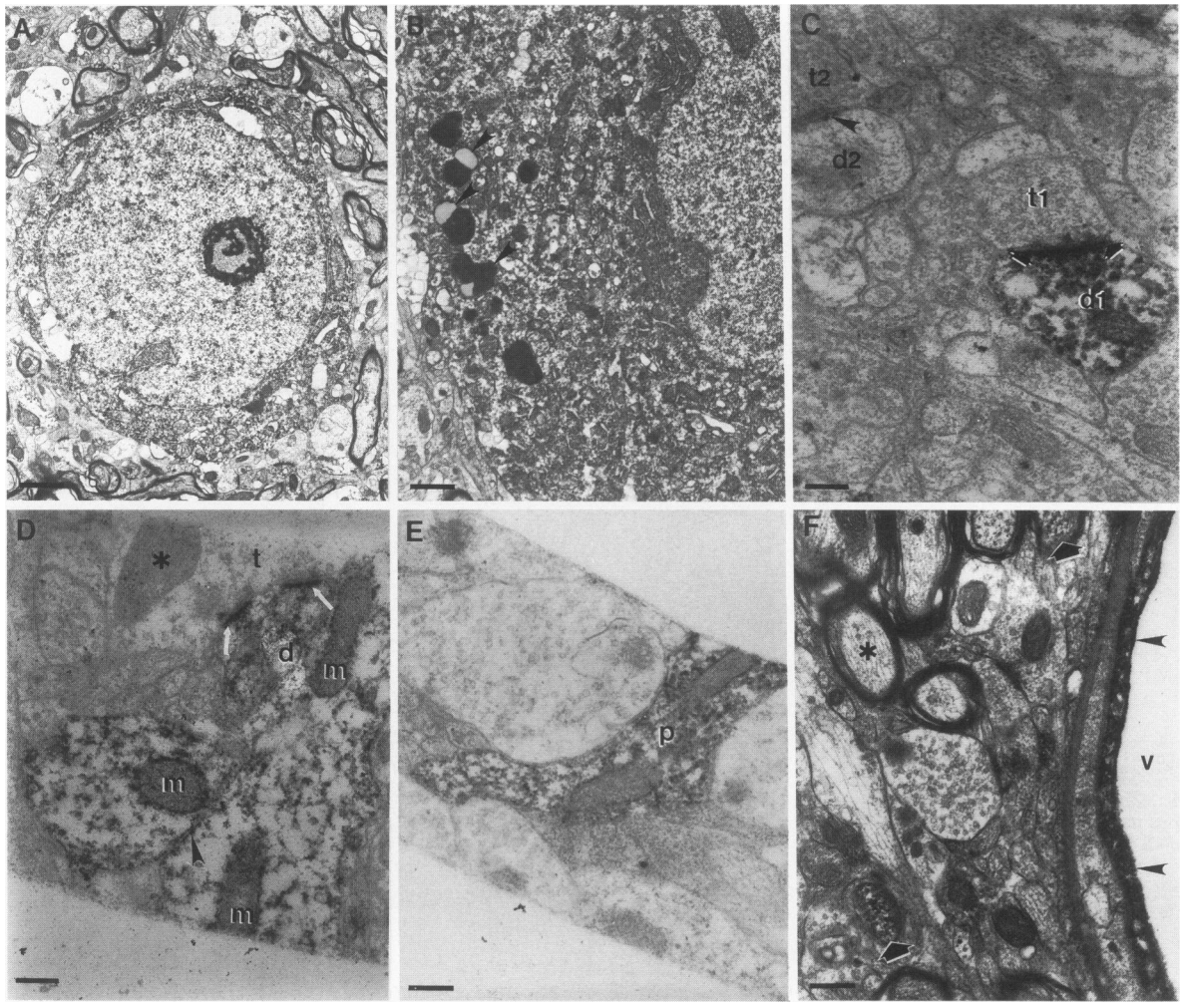

Figure 2. *Ultrastructural localization of APP within neuronal and nonneuronal cells.* (**A**) *APP-immunoreactive neuron in frontal cortex. Scale bar: 1.8 μ.* (**B**) *Portion of APP-immunoreactive neuronal perikaryon showing diffuse immunoreactivity within the cytoplasm, but lipofuscin granules (black objects with vacuole; arrowheads) show no immunoreactivity. Scale bar: 0.9 μ.* (**C**) *In the neuropil of cerebral cortex, APP immunoreactivity is enriched in a postsynaptic dendrite (d1) that forms an asymmetrical synapse with a nonimmunoreactive terminal (t1). APP immunoreactivity is aggregated at the postsynaptic density (arrows). Note the nonimmunoreactive symmetrical synapse (arrowhead) formed by dendrite (d2) and terminal (t2). Scale bar: 0.20 μ.* (**D**) *A dendrite (d) in hippocampus shows APP immunoreactivity distributed throughout the cytoplasm, with conspicuous aggregates associated with the plasmalemma (arrowhead), the outer membrane of mitochondria (m), and postsynaptic densities (white arrows). Nonimmunoreactive nerve terminal (t) with mitochondrion (asterisk) forms asymmetrical synapses with labeled dendrite (d). Scale bar: 0.19 μ.* (**E**) *APP-immunoreactive profile (p) in hippocampus could represent a process of a neuron or an astrocyte because of the absence of synaptic contacts on this process. Scale bar: 0.30 μ.* (**F**) *In cerebral cortex, endothelial cells (arrowheads) of subsets of capillaries (v) show APP immunoreactivity. Nearby APP-immunoreactive axons (broad arrows) and an unlabeled axon (asterisk) are present. Scale bar: 0.36 μ.*

polymorphic structures (50 to 100 μ in diameter) filled with numerous degenerating mitochondria as well as multilamellar and dense bodies. Some round organelles or degenerating profiles within swollen neurites were APP positive, but the ultrastructural identification of these profiles was equivocal. In most mature primitive plaques (Figure 3), it was difficult to discern if neurite-like, swollen cytoplasmic processes were dendritic, axonal, or glial in origin. The somata of neurons, microglia, and astrocytes were found within and at the periphery of senile plaques (see Figures 3, 8–11).

In three rhesus monkeys (ages 27, 29, and 31 years), early diffuse and mature plaques in layers I to III in the dorsolateral frontal and temporal cortices were evaluated ultrastructurally in detail to reconstruct the temporal formation of plaques. Early changes leading to plaque formation were characterized by single neurites surrounded by an intact neuropil (Figure 4). Dendrites (Figure 4A) and presynaptic axonal terminals (Figure 4B) participated in the formation of dystrophic neurites. In these early diffuse plaques, ICC localization of APP showed that early ultrastructural alterations at synapses occur without

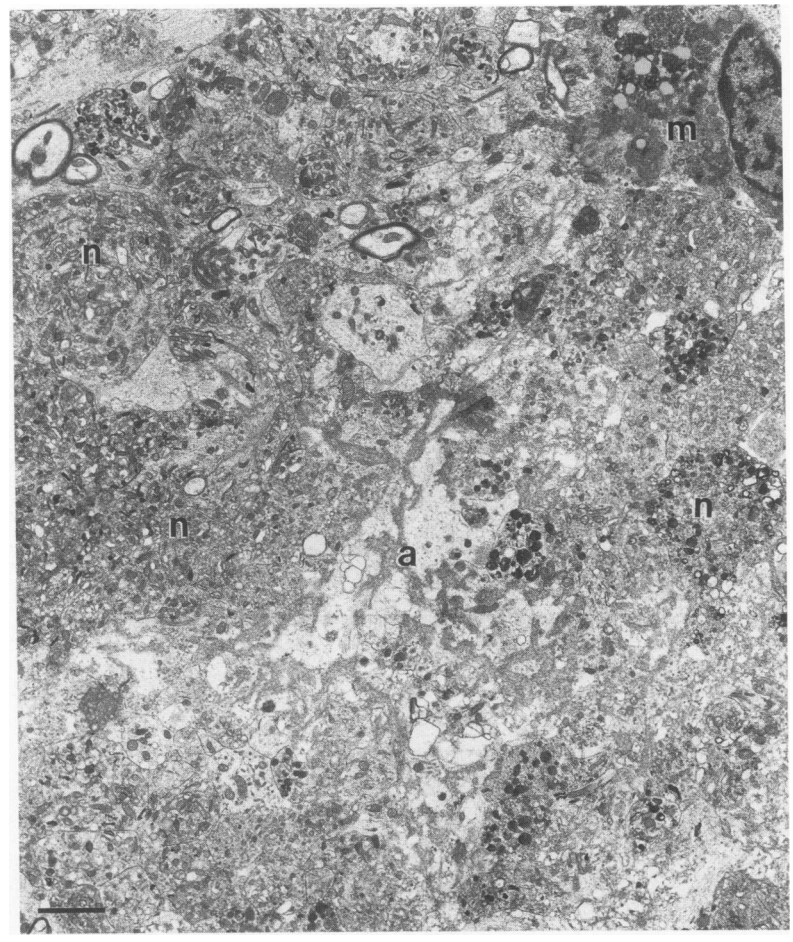

Figure 3. *Mature primitive senile plaque in the dorsolateral frontal cortex of a 31-year-old rhesus monkey shows the complexity of these lesions in the neuropil. A central area of extracellular amyloid (a) is surrounded by numerous, greatly enlarged neurites (n) filled with altered membranous organelles and a microglial cell (m). Scale bar: 1.25 μ.*

the accumulation of detectable APP within neurites, but, in mature primitive plaques, APP immunoreactivity was found accumulated within swollen neurites and in membranous inclusions within neurites. Moreover, ICC for Aβ and analysis of serial ultrathin sections revealed that synaptic abnormalities in early diffuse plaques occurred in the absence of detectable extracellular Aβ immunoreactivity and amyloid fibrils (Figure 4, C and D). There was also no evidence of sparse or scattered bundles of 8 to 10-nm amyloid fibrils between cell processes in early diffuse plaques, even after intensive evaluation at high EM magnifications. Occasionally, intracellular bundles of intermediate filaments could be misconstrued as amyloid fibrils if cytoplasmic membranes were disrupted. ICC analysis of serial sections through primitive plaques enriched in Aβ demonstrated the presence of APP. APP-enriched structures within plaques corresponded to dendrites (see Figure 7B), swollen axonal terminals, and, most frequently, reactive glial cells and their processes (see Figures 8C and 9A). Neuronal cell bodies and proximal dendrites, astrocytes, and microglia immunoreactive for APP, particularly the C-terminal epitope, clustered in the vicinity of plaques; in every plaque evaluated, APP-immunoreactive astrocytes and microglia and glial processes were found in immediate proximity to Aβ aggregates (see Figures 8–10).

Within most well-developed neuritic plaques, Aβ immunoreactivity was observed intracellularly within neuronal cell bodies (see Figure 6B), degenerating dendrites (see Figure 7, C and D), microglial cell bodies and processes (see Figure 11), and astroglial cell bodies and processes (Figures 5B, 6A). The colocalization of Aβ and CD68 as well as Aβ and GFAP revealed the frequent association of Aβ immunoreactivity with microglia and astrocytes, respectively. Immunoreactivity for Aβ was enhanced in sections pretreated with sodium borohydride. Aβ immunoreactivity within the extracellular compartment was fibrillar (Figure 5C). However, within the intracellular compartment, Aβ immunoreactivity occurred as nonfibrillar aggregates or granules and was associated with cell membranes (Figure 5B) and organelles of neurons and astrocytes (Figure 6, A and B) in primitive plaques. Immunoreactivity detected with antibodies

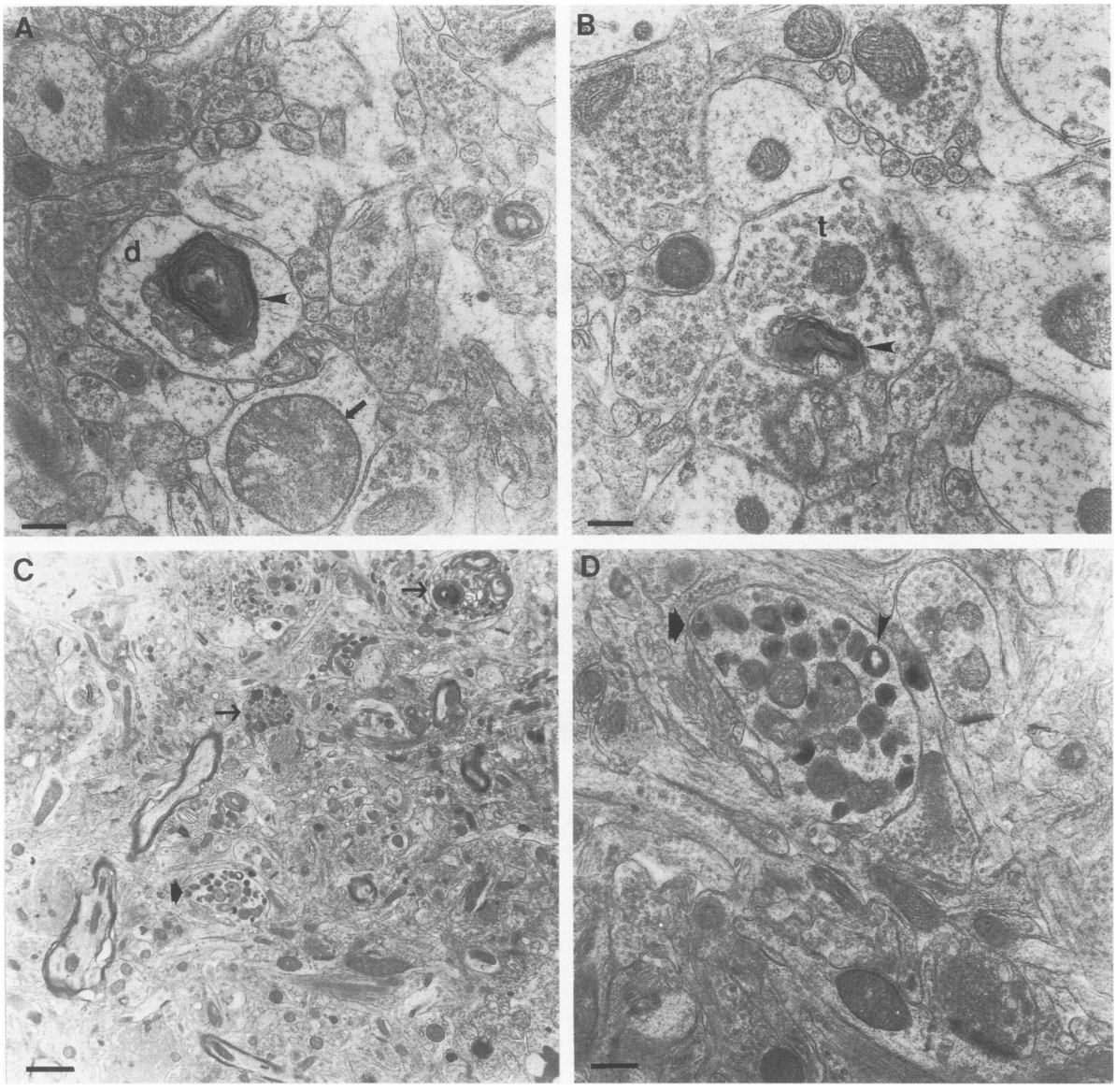

Figure 4. *Early ultrastructural changes in the cerebral cortex of macaques 26–29 years of age.* (**A**) *Early changes in dystrophic dendrites* (*d*) *include mitochondrial swelling* (*arrow*) *and the formation of dense, multilamellated, intradendritic inclusions* (*arrowhead*). *Scale bar: 0.30 μ.* (**B**) *Dense, multilamellated inclusions* (*arrowhead*) *are also present within dystrophic presynaptic terminals* (*t*). *Scale bar: 0.26 μ.* (**C**) *In early diffuse senile plaques, neuritic abnormalities* (*arrows*) *are often found in the absence of fibrillar amyloid. The broad arrow identifies a neurite seen at higher magnification in Figure 4D. Scale bar: 1.13 μ.* (**D**) *Neurite formed by dendrite* (*broad arrow*) *contains numerous degenerating mitochondria and dense, multilamellated bodies* (*arrowhead*). *Scale bar: 0.45 μ.*

to residues 1 to 28 of the Aβ region could be abolished by preadsorption of antibodies with synthetic Aβ (amino acids 1 to 28) (Figure 6C). No alterations in ICC staining patterns were observed when α-Aβ antibodies were preadsorbed against APP. In plaques, intracellular Aβ immunoreactivity decorated vacuoles of some lipofuscin granules within neuronal and glial cell bodies (Figure 6, A and B) and the cytoplasm of many abnormal dendrites (Figure 7C). Several examples of cytosolic accumulations of APP and Aβ immunoreactivities were encountered within dendrites at different stages of degeneration (Figure 7). Extensive dendritic degeneration and intradendritic accumulation of Aβ appeared to occur concomitantly with the formation of extracellular deposits of Aβ-immunoreactive fibrils (Figure 7D).

Glial cells and their processes were consistently present within plaques and Aβ deposits. By light microscopy, Aβ immunoreactivity colocalized with microglial (Figure 8, D and E) and astrocytic markers (Figure 9B). In serial 1-μ sections reacted with anti-Aβ antibodies and markers that identify microglia (CD68 or HLA-DR) and astrocytes (GFAP), cell bodies and processes of microglia and astrocytes were embed-

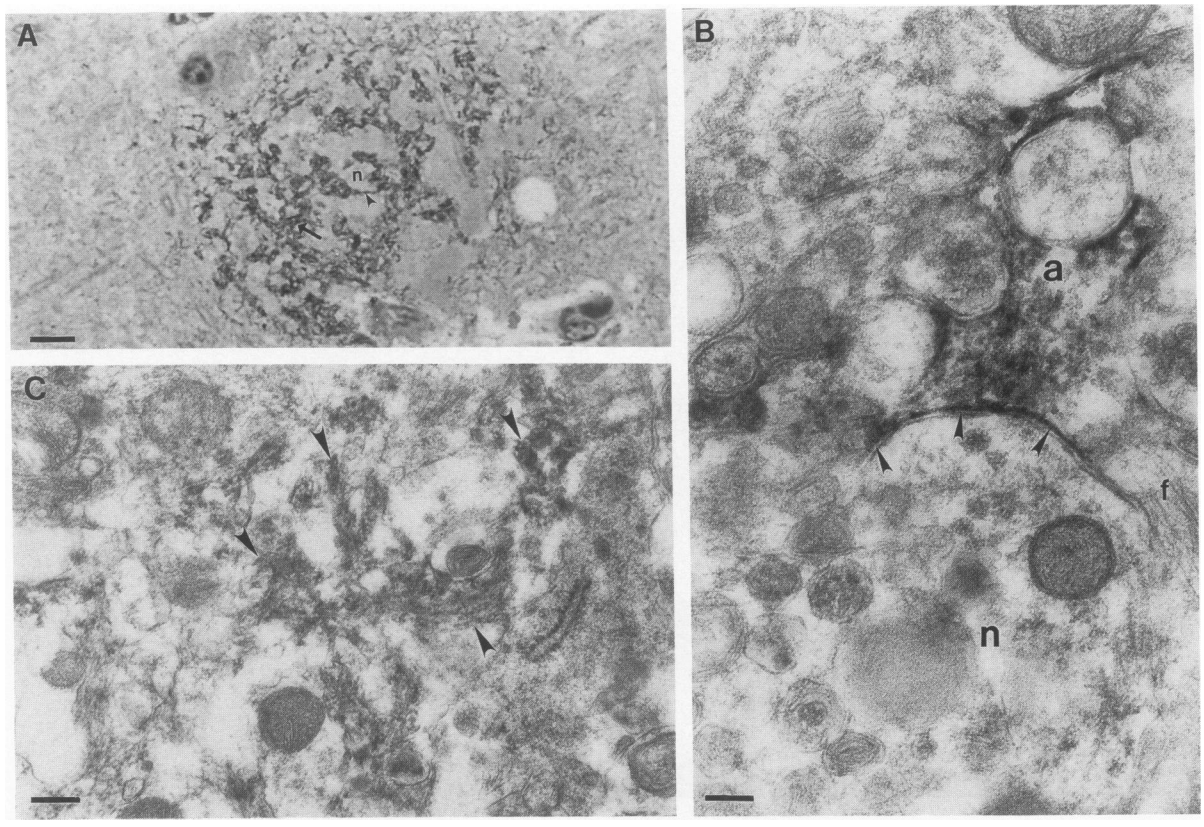

Figure 5. *Ultrastructural localization of Aβ in a primitive senile plaque within the frontal cortex of a 27-year-old macaque.* (A) *Toluidine blue counterstained semithin (1 μ) plastic section contains an Aβ-immunoreactive plaque. Aβ immunoreactivity is visualized as fine filamentous processes (arrowhead) surrounding neurites (n) and as apparent extracellular aggregates (arrow). Scale bar: 8.75 μ.* (B) *By EM, astrocytic processes (a) with bundles of intermediate filaments (f) show Aβ immunoreactivity. The plasmalemma of an Aβ-immunoreactive astrocytic process (arrowheads) is in direct apposition to an abnormal neurite (n). Scale bar: 0.6 μ.* (C) *Within the same plaque, Aβ immunoreactivity is also associated with extracellular fibrillar material (arrowheads). Scale bar: 0.36 μ.*

ded within the Aβ-immunoreactive neuropil (Figure 10). By EM, Aβ deposits within all plaques were closely associated with rod- or oval-shaped nonneuronal cell somata that contained numerous membrane-bound and free ribosomes and distended endoplasmic reticulum, suggesting that these cells were reactive microglia (Figure 11A). Within microglial cell bodies, some intracellular cisterns showed Aβ immunoreactivity (Figure 11B). Reactive microglia and astrocytes issued numerous processes that interdigitated with degenerating neurites and extracellular aggregates of amyloid fibrils. The evaluation of serial ultrathin sections revealed that spinous processes, originating from microglial cell bodies in the periphery of plaques, penetrated plaques and contained Aβ immunoreactivity (Figure 11C). In addition, some astroglial processes, identified by bundles of intermediate filaments, ensheathed neurites within plaques and expressed Aβ immunoreactivity (Figure 10, B and C). The cell bodies and processes of reactive astrocytes (but not resting astrocytes) within plaques often showed aggregates of Aβ immunoreactivity (Figures 9B and 10, B and C).

In aged monkeys, early diffuse and neuritic senile plaques showed increases in cytochrome oxidase and NADPH-diaphorase activity (Figure 12). Enhanced cytochrome oxidase activity was a consistent marker for early changes within plaques, as manifested by an increase in the activity of this enzyme within neurons and astrocytes in early plaques. Diffuse plaques positive for cytochrome oxidase (Figure 12C) occurred in the presence or absence of Aβ immunoreactivity. In neuritic plaques with diffuse deposits of Aβ, cytochrome oxidase activity was enriched within large, swollen neurites. As senile plaques became fully mature, cytochrome oxidase staining became aggregated (Figure 12D) and then reduced. Control sections from the brains of young and old monkeys incubated in the presence of potassium cyanide or in the absence of cytochrome C showed no cytochrome oxidase activity. NADPH-diaphorase activity was not located within neurites of senile plaques but was usually enriched diffusely within the neuropil of plaques (Figure 12A). Astrocytes and microglia and arborizing processes of these cells within early plaques with diffuse Aβ often showed positive

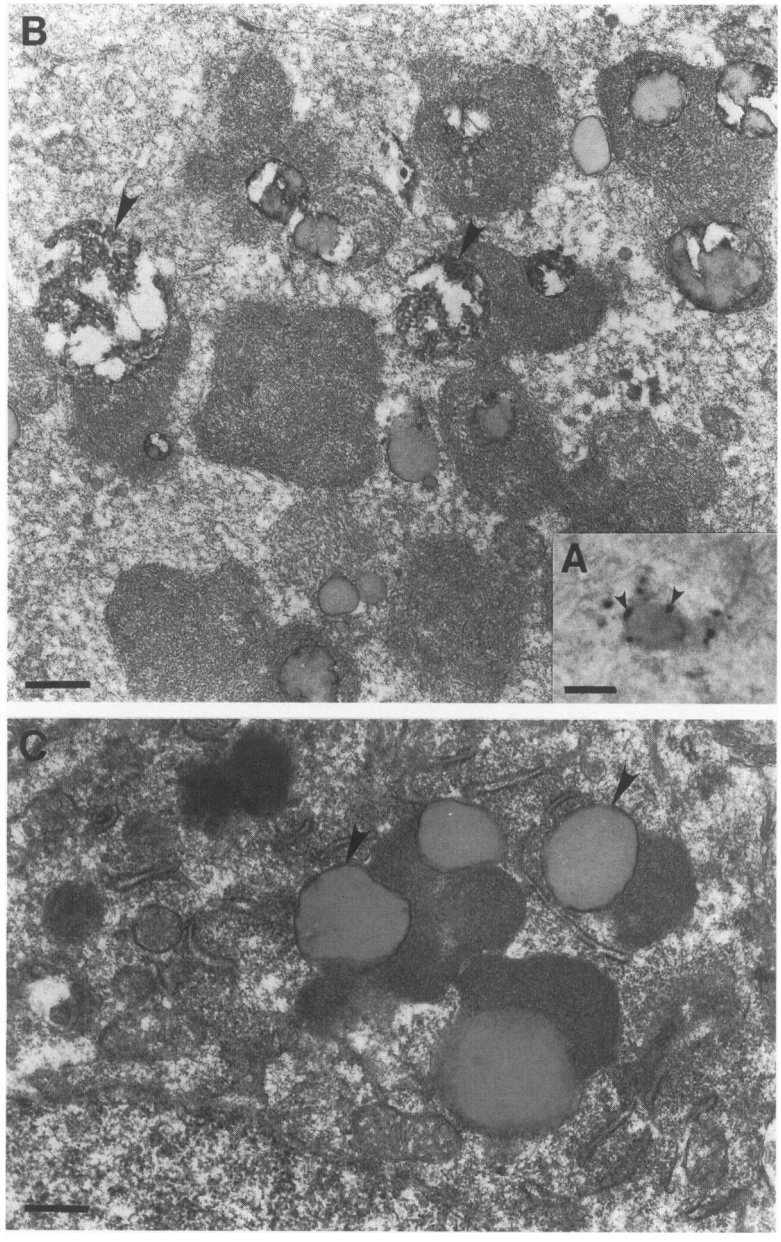

Figure 6. *Localization of Aβ within cells in dorsolateral frontal cortex of a lion-tailed macaque (>36 years of age).* (**A**) *A cell with a nuclear and cytoplasmic morphology of an astrocyte shows discrete granules of Aβ immunoreactivity at proximal processes and perinuclear sites (arrowheads). Scale bar: 7 μ.* (**B**) *Ultrastructural localization of Aβ immunoreactivity within vacuoles of perikaryal lysosomes or degenerating profiles (arrowheads) within a neuron in frontal cortex. Scale bar: 0.45 μ.* (**C**) *Control sections show an absence of Aβ immunoreactivity within lysosomal vacuoles (arrowheads). Scale bar: 0.45 μ.*

staining for NADPH-diaphorase. Control sections of brain incubated without NADPH or nitroblue tetrazolium showed no NADPH-diaphorase activity.

Neuritic plaques as well as Aβ and APP immunoreactivities were also associated with blood vessels within the cerebral cortex of some aged macaques (Figure 13). Capillaries in the vicinity of senile plaques were often surrounded by neurites (Figure 13B); many of these neurites were APP positive (Figure 13A). By EM, some capillaries showed Aβ immunoreactivity directly associated with the basement membrane and with astrocytic processes surrounding vessels. The colocalization of Aβ and GFAP as well as Aβ and CD68 revealed that Aβ-immunoreactive components of some blood vessels often corresponded to cytoplasmic processes of perivascular astrocytes (Figure 9C) and, less frequently, microglia (Figure 8F).

Discussion

The purpose of this study of the cerebral cortex of monkeys was twofold. The first aim, an extension of an earlier light microscopic study,[40] was to identify the cellular and subcellular localizations of APP and Aβ within the cerebral cortex in young and aged macaques. The second aim was to evaluate the cellular participants and evolution of structural abnormalities

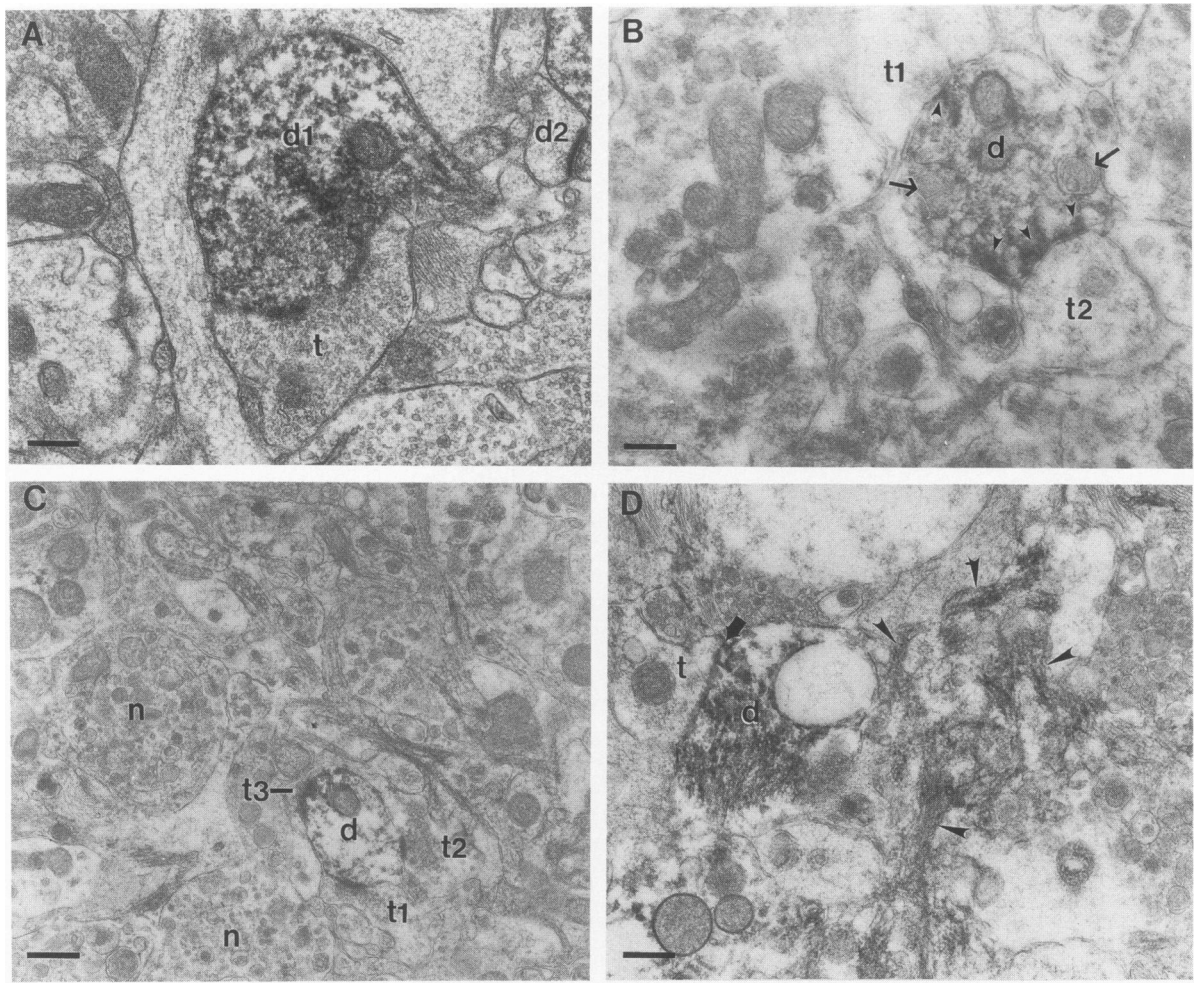

Figure 7. *Putative sequence of changes in the neocortical neuropil leading to the deposition of extracellular Aβ within senile plaques.* (A) *In normal cerebral cortex, APP immunoreactivity is enriched in subsets of dendrites (d1) that form synapses with nonimmunoreactive axonal terminals (t). The dendrite (d2) is not immunoreactive. Scale bar: 0.36 μ.* (B) *In the early stages of pathology in the cerebral cortex of an aged monkey, an abnormal dendrite (d) with degenerating mitochondria (arrows) shows intracellular aggregations of APP immunoreactivity (arrowheads) near the synaptic junctions formed at presynaptic terminals (t1 and t2). Scale bar: 0.36 μ.* (C) *In developing plaques that show neurites (n), subsets of dendrites (d) accumulate intracellular Aβ immunoreactivity, particularly near plasmalemmal sites postsynaptic to nerve terminals (t1, t2, and t3). Scale bar: 0.60 μ.* (D) *A degenerating dendrite (d) shows extensive cytoplasmic accumulation of Aβ immunoreactivity. A presynaptic nerve terminal (t) maintains an apparent synapse (arrow) with a degenerating dendrite. Aggregates of extracellular fibrillar Aβ (arrowheads) are nearby. Scale bar: 0.45 μ.*

that lead to the formation of plaques and Aβ deposits within the brains of monkeys during normal aging. These observations have implications for delineating the cellular pathology and events that lead to amyloidogenesis in the primate cerebral cortex during normal aging.

Localization of APP Within Cerebral Cortex

The precise cellular and subcellular localizations of APP in the brain are important for understanding the functions of APP and the mechanisms of amyloidogenesis as well as senile plaque formation. We have shown that APP is expressed by neural and nonneural cells, including subsets of pyramidal and nonpyramidal neurons, astrocytes, microglia, and vascular endothelial cells and pericytes in the cerebral cortex. In normal brain, the most prominent neuronal localization of APP is within cell bodies and dendrites; furthermore, APP is particularly enriched postsynaptically at subsets of synapses. By *in situ* hybridization, mRNA transcripts for APP were found to be expressed in neuronal perikarya in the brains of rats,[49] monkeys,[50,51] and humans.[50–52] Light microscopic ICC studies have shown that APP immunoreactivity is localized to neurons and their processes in several brain regions.[40,49,53–58] Ultrastructural studies show that APP is localized presynaptically in axonal terminals within the rodent central and peripheral nervous

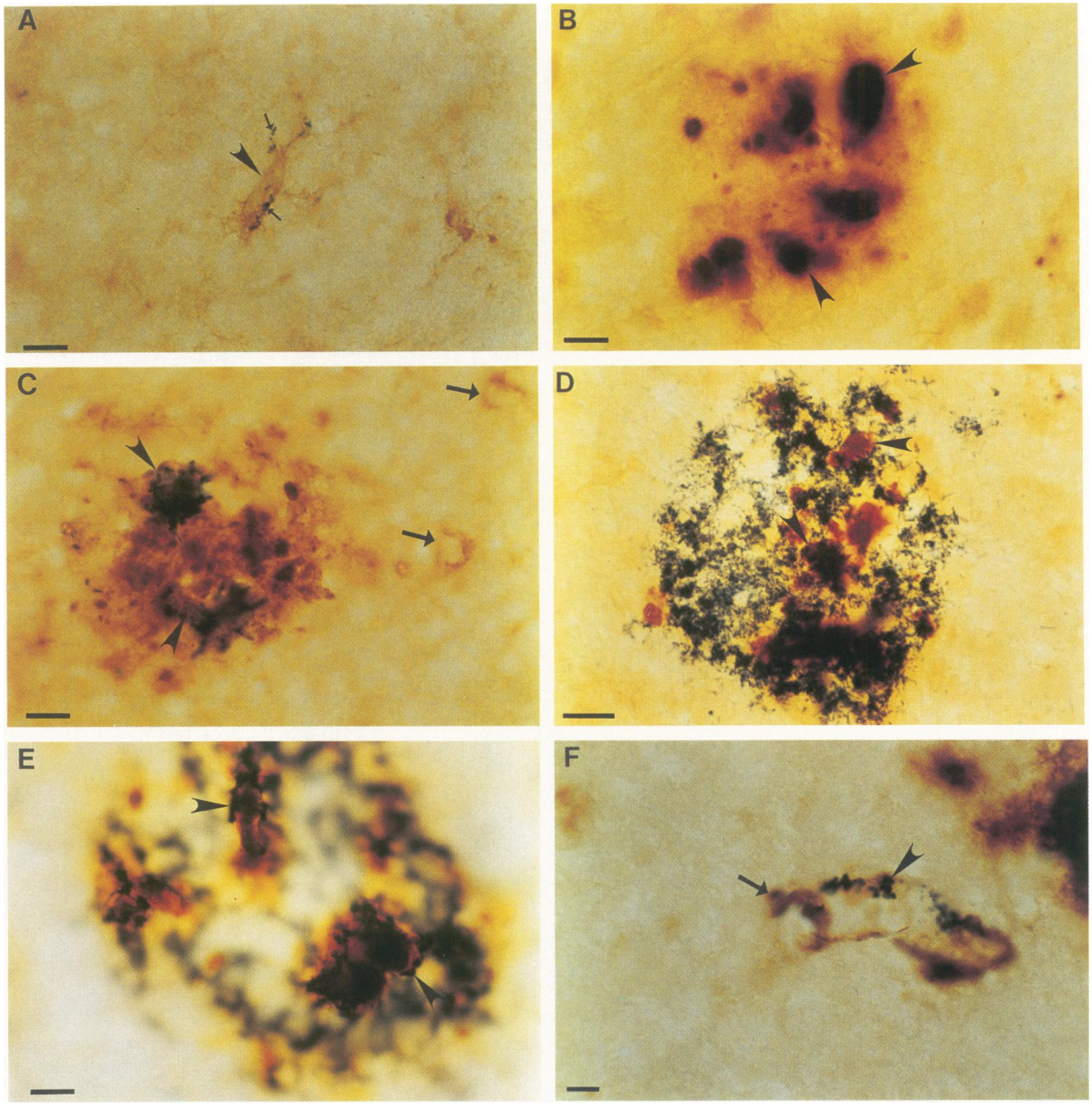

Figure 8. *Microglia express APP and Aβ.* (**A**) *A resting microglia cell (arrowhead), identified by particulate CD68 immunoreactivity (black-green at small arrows), shows low APP immunoreactivity (brown). Scale bar: 11.5 μ.* (**B**) *A senile plaque in the frontal cortex of an aged (29-year-old) monkey contains several large, globoid, CD68-immunoreactive, activated microglial cells (arrowheads). Scale bar: 11.25 μ.* (**C**) *Activated microglia within this senile plaque are enriched in APP immunoreactivity (arrowheads) as demonstrated by the colocalization of CD68 immunoreactivity (black-green) and APP immunoreactivity (brown). APP-immunoreactive neurons (arrows) are present. Scale bar: 12 μ.* (**D**) *This Aβ-immunoreactive plaque (black-green) contains several CD68-immunoreactive microglia (brown). Some of these microglial cells colocalize within Aβ immunoreactivity (arrowheads). Scale bar: 11.7 μ.* (**E**) *Focusing on microglial cell bodies (brown) in the z-axis of this plaque reveals that microglia have Aβ immunoreactivity (black-green) on or near their surfaces (arrowheads). Scale bar: 10 μ.* (**F**) *This Aβ-immunoreactive capillary (arrow) contains CD68-immunoreactive perivascular cells (arrowhead). Scale bar: 10 μ.*

systems.[59] However, our study of monkey brain and another EM investigation of rat brain[60] demonstrate that, at synapses, APP is predominantly localized postsynaptically within dendrites and dendritic spines of subsets of asymmetrical synapses. Moreover, our observations show that APP is associated with postsynaptic densities as suggested by another study.[60] Because the antibodies used in this study were not selective for specific APP isoforms, we cannot address the possible differential localizations of these APP isoforms, including the forms containing the Kunitz protease inhibitor domains.

The expression of APP within nonneuronal cells in brain has been controversial. ICC studies of rat brain have reported APP-immunoreactive astrocytic processes surrounding neurons and blood vessels in ce-

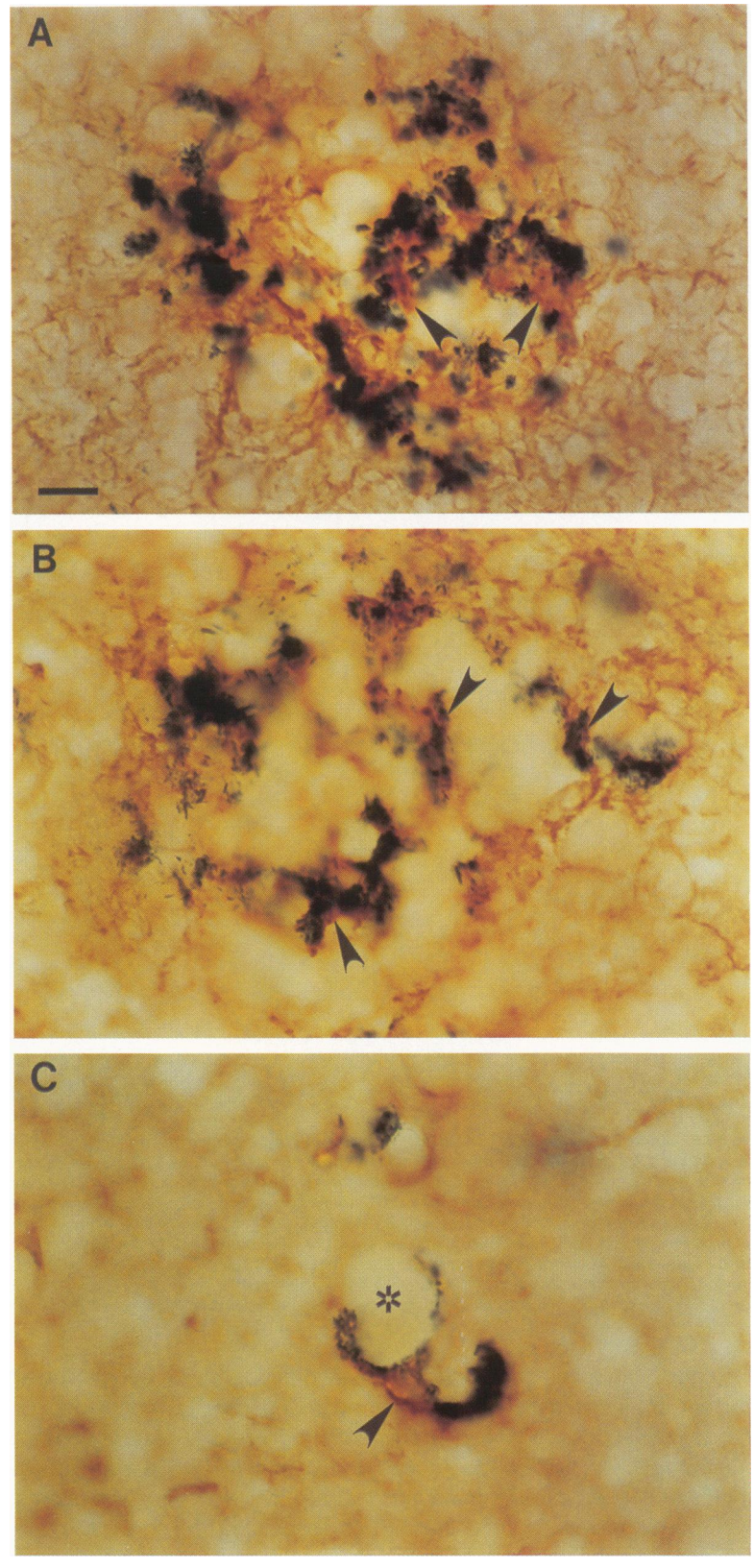

Figure 9. *Astrocytes express APP and Aβ. Scale bar: 10 μ.* (**A**) *Some GFAP-positive elements (brown) in this APP-enriched plaque (black-green) are immunoreactive for APP (arrowheads). The surrounding neuropil displays a reticular network of single-labeled astrocytic processes (brown).* (**B**) *Astrocytic processes, identified by GFAP immunoreactivity (brown), within this Aβ-positive plaque (black-green) are Aβ immunoreactive (arrowheads). Single-labeled astrocytic processes form a reticular network in the surrounding neuropil (brown).* (**C**) *This cerebral microvessel (asterisk) is enveloped by an astrocyte (arrowhead) identified by GFAP immunoreactivity (brown). This perivascular astrocyte is Aβ immunoreactive (black-green).*

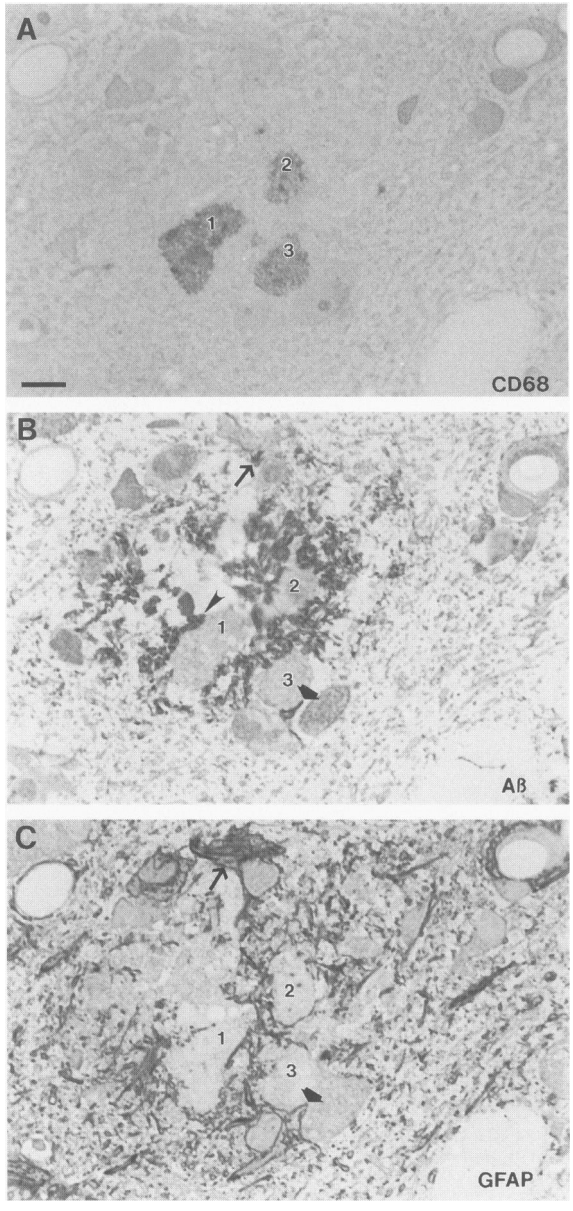

Figure 10. *Postembedding ICC on adjacent 1-μ-thick plastic sections of the same senile plaque shows the spatial relationships between microglia* (**A**), *Aβ* (**B**), *and astrocytes* (**C**). *Numbers* (*1, 2, and 3*) *identify the same cells in all three sections of the plaque.* (**A**) *Three microglial cells identified by CD68 immunoreactivity are found within this plaque at this plane of section. The somata of these three microglial cells are immunonegative for Aβ* (*Figure 10B*), *but the Aβ envelopment of these cells may correspond to microglial processes that are poorly labeled by CD68 antibodies. Scale bar: 7.5 μ.* (**B**) *Aβ immunoreactivity is in immediate proximity to surfaces of microglial cells* (*arrowhead*). *Some processes that surround microglial cells* (*broad arrow*) *are Aβ immunoreactive and correspond to astrocytic processes* (*broad arrow in* **C**). *Some cell bodies that are Aβ immunoreactive* (*thin arrow*) *correspond to astrocytes* (*thin arrow in* **C**). *Scale bar: 7.5 μ.* (**C**) *Localization of GFAP immunoreactivity shows that reactive astrocytes are located within or at the periphery of plaques, and numerous astrocytic processes infiltrate into plaques. Astrocytic cell body* (*thin arrow*) *shows GFAP-positive cytoplasm and a large immunonegative nucleus. Some GFAP-positive astrocytic elements* (*broad and thin arrows*) *colocalize with Aβ immunoreactivity* (*broad and thin arrows in B*). *Scale bar: 7.5 μ.*

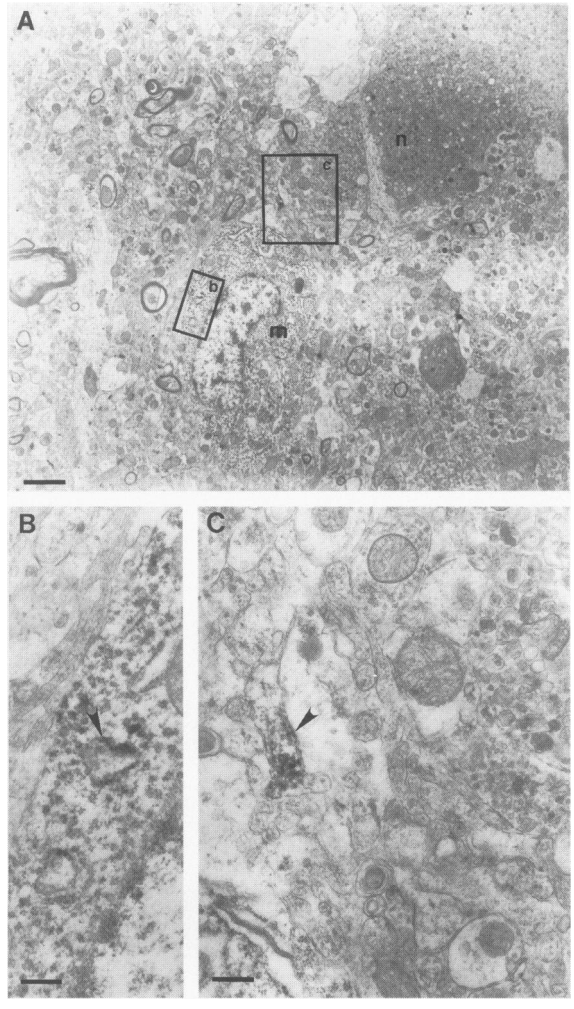

Figure 11. *EM shows that microglia within senile plaques are Aβ immunoreactive.* (**A**) *A microglial cell* (*m*) *found within a plaque containing dystrophic neurites* (*n*) *and Aβ. Outlined areas* (*b and c*) *are shown at higher magnification in B and C. Scale bar: 1.29 μ.* (**B**) *Cisterns within the cytoplasm of microglial cells show Aβ immunoreactivity on the surface. Scale bar: 0.60 μ.* (**C**) *Aβ-immunoreactive spiny processes of microglial cells are found within plaques. Analysis of serial ultrathin sections revealed that this process was continuous with a primary process of a microglial cell. Scale bar: 0.45 μ.*

rebral cortex,[53] but endothelial cells of the cerebral vasculature were not immunoreactive.[53] APP-expressing glial cells were not observed in rodent brain in another ICC study.[49] *In situ* hybridization and ICC studies of human brain suggest similar discrepancies.[52,55,61,62] *In vitro* data show that astrocytes and microglia express the major isoforms of APP.[63] Our study of monkey brain demonstrates that nonneuronal cells (ie, astrocytes, microglia, and endothelial cells) express APP. The abundance of APP-immunoreactive nonneuronal cells in brain is low in comparison with the dominant expression of APP within neurons and their processes, and it appears that astrocytes and microglia constitutively express APP at low levels in the resting state. However, the

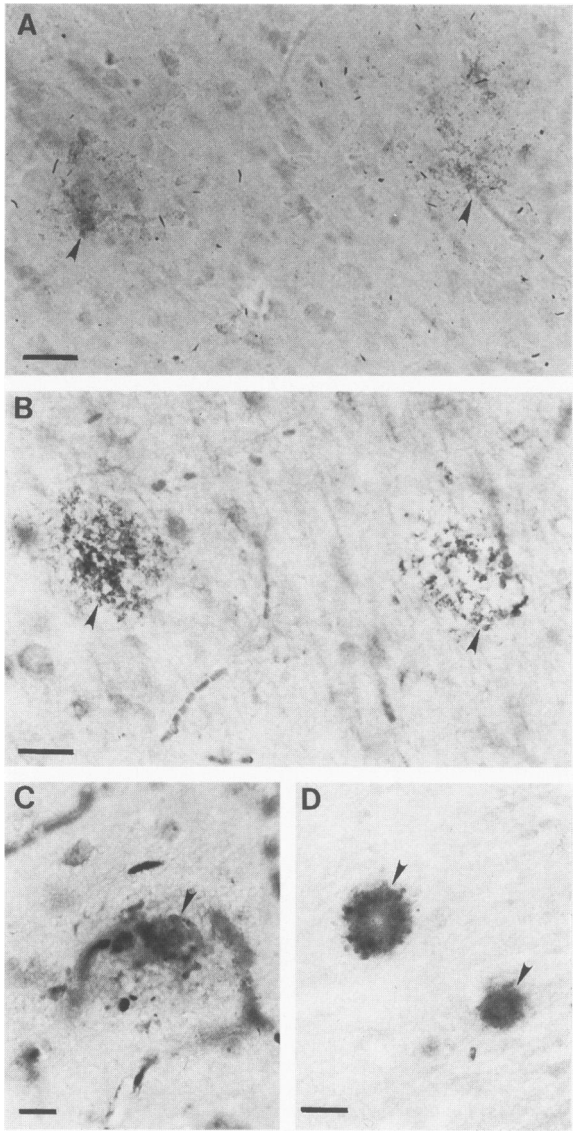

Figure 12. *Histochemical localization of NADPH-diaphorase* (**A**) *and cytochrome oxidase* (**C, D**) *activities within neocortical senile plaques.* (**A, B**) *In adjacent sections, NADPH-diaphorase activity is localized diffusely in the neuropil of plaques* (*arrowheads in* **A**) *that contain Aβ immunoreactivity* (*arrowheads in* **B**). *In this photomicrograph* (**A**), *diaphorase-positive nonpyramidal neuronal cell bodies are not present. Scattered dark crystals are background. Scale bars: 25.8 μ.* (**C**) *In early plaques, large swollen neurites are enriched in cytochrome oxidase activity* (*arrowhead*). *Surrounding capillaries are also enriched in cytochrome oxidase. Scale bar: 18.8 μ.* (**D**) *In plaques* (*arrowheads*) *more mature than the plaque shown in* **C**, *cytochrome oxidase activity is very dense in neurites within the parenchyma. Scale bar: 37.5 μ.*

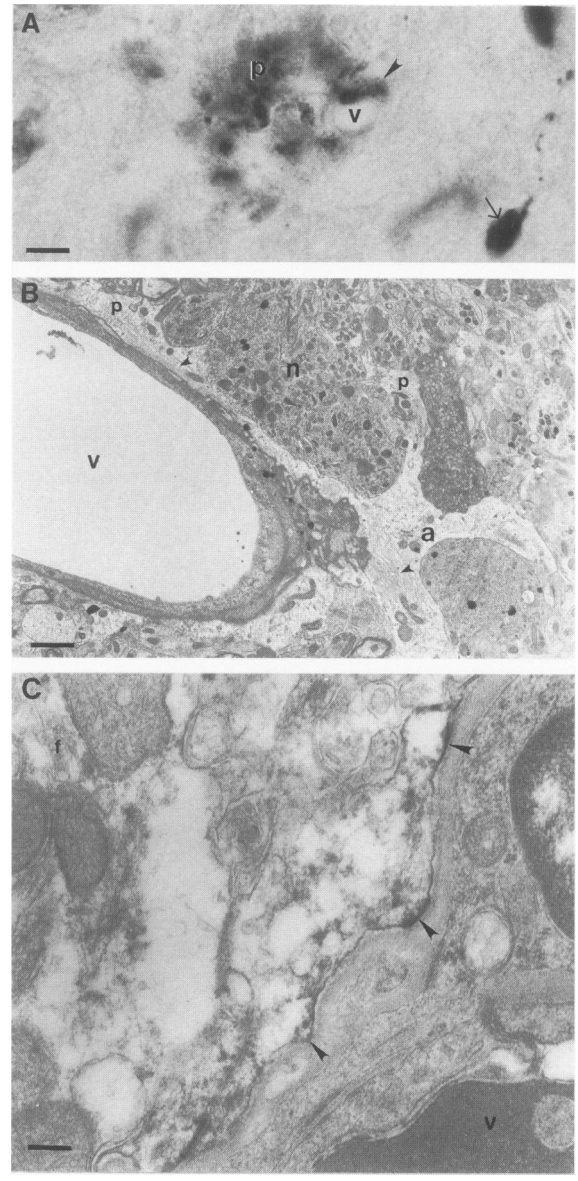

Figure 13. *Associations between neurites, astrocytes, Aβ immunoreactivity, and blood vessels.* (**A**) *A plaque* (*p*) *enriched in APP immunoreactivity* (*visualized with antibody CT15*) *is close to a blood vessel* (*v*). *An APP-immunoreactive neurite* (*arrowhead*) *is closely apposed to the vessel. Note the other APP-enriched neurite* (*thin arrow*). *Scale bar: 50 μ.* (**B**) *EM shows that a neurite* (*n*) *of a senile plaque is separated from a blood vessel* (*v*) *by processes* (*p*) *of an astrocyte* (*a*) *containing bundles of intermediate filaments* (*arrowhead*). *Scale bar: 1.50 μ. C. Astrocytic process that envelops a blood vessel* (*v*) *shows Aβ immunoreactivity at the plasmalemma* (*arrowheads*). *Intermediate filaments* (*f*) *are seen in the upper left. Scale bar: 0.36 μ.*

relative enrichment of APP within these nonneuronal cells may change in response to synaptic abnormalities that occur during aging. This idea is supported by our finding that APP is expressed prominently by activated astrocytes and microglia within plaques in aged monkey brain and by other EM reports[64] showing that APP is localized to astrocytes in senile plaques in cases of AD. Further support for our results is found in studies showing that APP isoforms containing the Kunitz protease inhibitor domain are expressed in reactive astrocytes in early stages of brain damage.[56] Because levels of APP in some neurons and nonneuronal cells are increased by interleukin-1,[65] it is likely that the expression of APP is inducible

in glia when these cells are transformed from a resting state to an activated state.

In postmortem brain tissue from control humans, ICC studies of non-Aβ regions of APP have yielded conflicting results. In normal human brain, cortical neurons, astrocytes, and blood vessels are APP positive.[55] CA1 neurons of hippocampus are immunoreactive,[54] and APP is thought to be concentrated in neuronal lysosomes (see Figure 4 in Benowitz et al.[54]). For the most part, our present and previous results[40] on the cellular localization of APP in nonhuman primate brain are consistent with studies of human brain. However, we were unable to confirm the localization of APP within neuronal lysosomes. Although electron-dense organelles that resemble lysosomes and lipofuscin granules were identified within the cytoplasm of neuronal perikarya in monkey brain, these organelles did not show specific immunoreactivity for APP in sections incubated with three different anti-APP antibodies compared with sections incubated with control sera. Several other immuno-EM localization studies of APP in the central nervous system of experimental animals have also failed to document the presence of APP in neuronal lysosomes *in vivo*.[53,59,60,66] These discrepant results between optimally prepared animal and postmortem human brains may be caused by differences in the anti-APP antibodies used or by artifactual, autolytic changes in postmortem human brain. However, we did visualize Aβ immunoreactivity within neuronal lysosomes/lipofuscin granules, suggesting that Aβ is incorporated into these organelles but not derived from APP within these structures or that APP within lysosomes is processed rapidly so that antigenicity is lost. Furthermore, the antipeptide antibody to Aβ used in this study immunolabels structures that were not labeled with three APP antibodies that recognized different epitopes of the molecule. Aβ immunoreactivity was not diminished by competition with APP; thus, it is likely that this α-Aβ antibody is not cross reacting with full-length APP.

The functions of APP are not well defined. Secreted and nonsecreted forms of APP exist.[67,68] APP has structural features similar to some cell surface receptors.[15] In addition, APP is incorporated into the extracellular matrix[69] and may have roles in cell-cell and cell-substrate adhesion.[49,67,70–72] Furthermore, APP may function in the regulation of neurite outgrowth[73,74] perhaps by mediating the effects of nerve growth factor,[75] in the morphogenesis of neural[76] and nonneural[61] tissues, and in neuronal and glial responses to brain injury.[36,56,77] Although APP is a ubiquitous protein within neurons throughout the brain in several species of animals, different populations of cells may differentially regulate the expression of APP at perikaryal and synaptic levels. Most, if not all, neurons within specific cortical laminae and hippocampal subfields contain mRNA for APP,[50,51] whereas ICC shows that neocortical and hippocampal neurons exhibit varying cytoplasmic accumulations of APP immunoreactivity.[40] As is the case for numerous brain neuropeptides and neurotrophic factors,[78–81] the posttranslational expression of APP in distinct populations of neurons and at synapses may be regulated differentially by activity-dependent mechanisms (ie, transsynaptic activation by neuronal afferents) or by factors within the synaptic microenvironment. For example, expression of the APP gene is regulated by cell- or tissue-specific factors that may modulate the synthesis of APP.[82] However, we know little about the posttranslational kinetics of APP metabolism *in vivo*. Our data, which demonstrate synaptic and reactive glial localizations of APP, are consistent with evidence indicating that APP has an important function in cell adhesion and in the plasticity of neurons and supporting cells. It is possible that APP within neurons and glia has a role in the steady-state dynamics of synaptic contact formation, stabilization, and maintenance within the immature, mature, and aged brain.

Formation of Senile Plaques and Aβ Deposits Within the Aging Cerebral Cortex

Differences and similarities exist between the formation and distribution of age-related neuropathology in nonhuman primates and humans. In the present study, senile plaques were found most frequently in frontal (dorsolateral and orbital) and temporal (superior) neocortex, whereas entorhinal cortex and hippocampus were relatively spared during the aging process in nonhuman primates. Neurofibrillary tangles are not formed in these animals. Most mature plaques in these aged macaques are classified as diffuse or primitive and contain Aβ immunoreactivity. The early diffuse plaques, defined ultrastructurally as focal abnormalities in synaptic morphology of the neuropil, were devoid of amyloid fibrils and Aβ immunoreactivity. These early diffuse plaques identified in the present study are seemingly precursors of mature diffuse plaques with Aβ deposits. Classic (with central amyloid cores) and compact plaques occurred less frequently than diffuse plaques in the neocortex in aged monkeys. In normal aged nondemented humans, diffuse and primitive plaques with Aβ immunoreactivity are quantitatively the prevalent

lesions found in neocortical regions (eg, frontal and superior/middle temporal cortex) but not in hippocampus.[83–86] In contrast, in individuals with AD, diffuse, primitive, classic, and compact senile plaques as well as neurofibrillary tangles occur in a variety of neocortical regions and in hippocampus.[87] We conclude that mechanisms for the formation of diffuse senile plaques and Aβ deposits are similar in aged monkeys and normal elderly humans, but mechanisms (possibly involving paired helical filaments) for the formation of classic plaques and neurofibrillary tangles differ in normal aging as compared with AD. Unfortunately, EM studies of diffuse and primitive plaques in autopsy tissue from cognitively characterized, nondemented elderly individuals have not been done, but EM studies of senile plaques in AD brain are available for comparison.

Earlier EM reports are discrepant regarding the cellular dynamics and temporal evolution of amyloid deposition within senile plaques.[10,37,88–90] Plaques contain degenerating neuronal cell bodies and neurites (ie, abnormal presynaptic nerve terminals and dendrites), reactive astrocytes and microglia, microvessels, and aggregates of amyloid fibrils.[9,10,91,92] Thus, it is understandable that several hypotheses of senile plaque formation and amyloid deposition have been promulgated. The genesis of senile plaques may begin with the formation of extracellular amyloid before the degeneration of cellular elements within plaques.[89,93] Alternatively, Aβ may be derived from degenerating axonal nerve terminals or dendrites containing APP that evolve into neurite-rich foci that form Aβ at the plasmalemma by aberrant processing of APP,[35,40,94] invading reactive microglia that actively produce Aβ,[10,37,95] or capillary or serum-derived APP.[43,92] Specifically, in one scheme for senile plaque formation, amyloid (in a nonfibrillar form and then a fibrillar form) is deposited before neuritic degeneration;[90,96] in diffuse plaques, Aβ may be formed by amyloid-related cells and processes[90,97] that are possibly astrocyte derived.[97] In our EM preparations from several aged monkeys, we did not identify extracellular amyloid (even as sparse, scattered bundles of fibrils) before the appearance of synaptic abnormalities and dendritic/axonal neurites. Our EM observations on early diffuse plaques thus differ from the results seen in AD brain.[89] The lack of evidence for extracellular amyloid fibrils in early diffuse plaques in this study may be accounted for by our evaluation of plaques at an earlier stage of maturation than plaques evaluated by others.[89] However, in diffuse plaques, we did identify Aβ-immunoreactive transformed astrocytes and microglia corresponding to previously shown amyloid-related cells.[90,97] Our EM data and the interpretation of these results in aging nonhuman primates are most concordant with ultrastructural studies of senile plaques in cerebral cortex from cases of AD and aged monkeys conducted by Wisniewski and coworkers.[10,37,88] In these studies, senile plaques were envisioned to be dynamic lesions that evolve from primitive plaques to mature plaques; the sequencing of degenerative changes was thought to be the degeneration of neuritic structures, followed by the attraction of reactive glia, and the subsequent deposition of extracellular amyloid derived from microglia.[10,37] Our observations favor the view that morphological and biochemical perturbations within neuronal and nonneuronal cells occur before the deposition of extracellular Aβ fibrils. Furthermore, our results suggest that focal abnormalities in neuron-neuron synaptic contacts within the neuropil (synaptic disjunction) may incite this complex series of events resulting in the formation of diffuse senile plaques and deposits of amyloid.

On the basis of our present data, we have tentatively reconstructed the temporal and spatial events that lead to the formation of plaques and Aβ in the cerebral cortex (Figure 14). Synaptic abnormalities are early events in plaque formation and take place before the accumulation of intracellular and extracellular APP and Aβ (Figure 14, A and B). This conclusion is supported by our observations showing that alterations in the fine structure of both pre- and postsynaptic neuronal processes occur within the neocortical neuropil to form early diffuse plaques. These synaptic changes were defined by the formation of inclusions and degenerating profiles within presynaptic and postsynaptic elements, possibly reflecting mitochondrial degeneration. Our observations showing enhanced cytochrome oxidase activity in early diffuse senile plaques could be interpreted as a mitochondrial functional impairment with a compensatory augmentation in cytochrome oxidase activity early in these lesions. Alternatively, increased cytochrome oxidase staining in early senile plaques may reflect activation of glial cells. In response to synaptic disjunction, neuritic abnormalities may occur to form primitive senile plaques (Figure 14, B and C). These neurites, formed by dendrites and nerve terminals, accumulate full-length APP and eventually intracellular, perhaps soluble, Aβ (Figure 14C). The accumulation of APP within neurites of neocortical plaques in aged monkeys[40] and in cases of AD[26,61,98–101] is consistent with observations in the peripheral nervous system showing that APP is transported anterogradely in axons[102,103] and that nerve injury increases the cellular expression of APP mRNA.[104] Occurring concomitantly with synaptic disjunction and

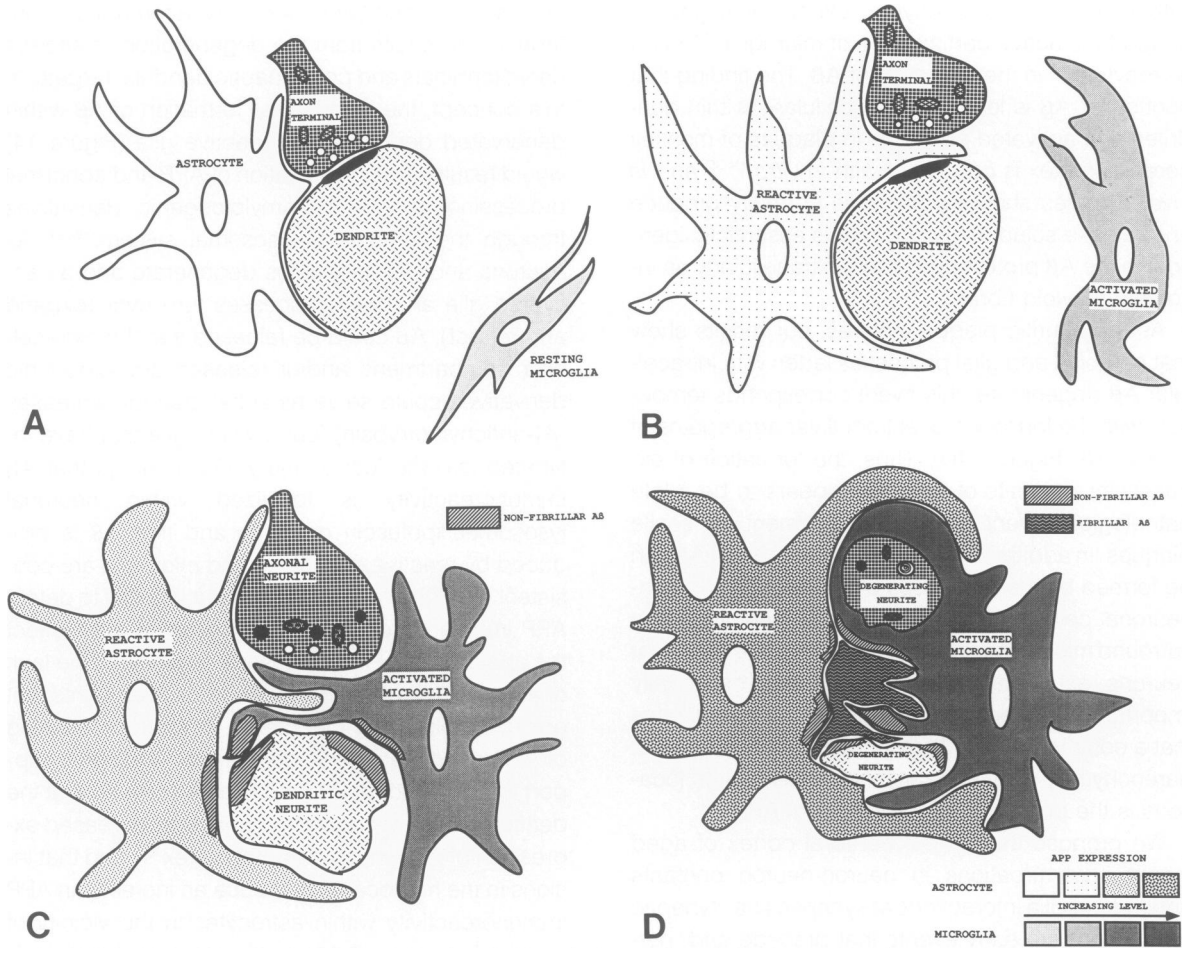

Figure 14. *Schematic diagram depicts the possible temporal and spatial sequence of events that lead to senile plaque formation and parenchymal deposits of Aβ.* (**A**) *Simplified synaptic organization in normal cerebral cortex as represented by an axon terminal (with synaptic vesicles and mitochondria) forming an asymmetrical synapse with an APP-enriched dendritic profile seen in cross section. An astrocyte partially envelops the synapse, and a resting microglial cell is found in the surrounding neuropil.* (**B**) *At an early stage in the formation of early diffuse senile plaques, these important events occur: synaptic disjunction (ie, separation of pre- and postsynaptic elements), possibly caused by impairments in mitochondrial functioning or cell-cell contact; transformation of astrocyte and microglia to an activated state; and up-regulation of APP expression in activated glial cells. Astrocytic processes invade the synaptic cleft and begin to isolate the disconnected axon terminal (forming dense bodies) and dendrite. An activated microglial cell migrates toward the abnormal synapse, possibly in response to secreted factors from an astrocyte or damaged nerve terminal/dendrite.* (**C**) *Axonal and dendritic neurites (containing degenerating mitochondria and dense bodies) are formed within diffuse plaques. An APP-enriched activated microglial cell begins to envelop dystrophic neurites, and an APP-enriched reactive astrocyte isolates the abnormal focus within the brain parenchyma. Dendritic neurite, astrocyte, and microglial cells accumulate intracellularly nonfibrillar Aβ.* (**D**) *Within primitive plaques, degenerating neurites (containing degenerating mitochondria and dense multilamellated bodies) are phagocytosed more completely by activated microglia, and the site of parenchymal injury is partially isolated by reactive astrocyte. Intracellular, nonfibrillar Aβ (formed by reactive astrocyte, activated microglia, and degenerating neurites) is released/secreted into the extracellular compartment and aggregates as β-pleated fibrils.*

incipient degeneration of neurites derived from neuronal processes is the transformation of resting astrocytes and microglia to activated glia and the increased expression of APP within these cells (Figure 14, A–C) or increased uptake of extracellular APP by these cells. Synaptic changes may provoke increased APP expression in neuronal and glial cells through factors released from degenerating dendrites or axonal terminals. Some molecular signals may be factors such as calcitonin gene-related peptides[105] or complement proteins.[106] Activated APP-enriched microglial and astrocytic processes infiltrate into neuritic foci and produce intracellular nonfibrillar Aβ (Figure 14, B and C). The precise cytosolic proteolytic events that form Aβ from APP are uncertain, but calcium influx into neuronal or glial elements and the subsequent activation of calcium-stimulated cysteine or serine proteases may be involved.[38,107,108]

Enzyme histochemistry shows that, within immature plaques, astrocytes and microglia express NADPH-diaphorase, a nitric oxide synthase.[109] Thus, reactive glial cells may synthesize and secrete focally diffusible agents that promote cellular injury and resorption of damaged dendrites and nerve terminals

within the brain parenchyma. Other investigations support the active participation of microglia[37,95] and astrocytes[110] in the formation of Aβ. The finding that nonfibrillar Aβ is localized intracellularly within dendrites and activated glial cells in plaques of monkey cerebral cortex is consistent with *in vitro*[28–30] and *in vivo*[29] studies showing that cells normally produce and release soluble 4-kd Aβ that is essentially identical to the Aβ protein deposited extracellularly as insoluble amyloid fibrils.

As the neuritic plaque matures, our results show that neuronal and glial processes laden with intracellular Aβ degenerate; this event corresponds temporally with the formation of extracellular aggregates of fibrillar Aβ (Figure 14D). Thus, the formation of extracellular deposits of amyloid appears to be a late pathological event in the development of senile plaques. In addition, we provide evidence that Aβ can be formed by the processes of APP-containing nonneuronal cells (astrocytes, microglia, pericytes) that surround microvessels within cerebral cortex and that neurons, astrocytes, and microglia may be equally important for Aβ deposition. Our study also indicates that a common mechanism for the formation of Aβ at parenchymal, perivascular, and white matter locations is the derivation of Aβ from glial APP.

We propose that, in the cerebral cortex of aged monkey, perturbations in neuron-neuron contacts and neuron-glia interactions at synapses (ie, synaptic disjunction) are early events that precede and, perhaps, lead to the formation of senile plaques and Aβ deposits (Figure 14). Quantitative studies of cerebral cortical synapses in normal aged individuals[111–113] and in individuals with AD[114–118] have shown significant losses of synapses that may occur at an early stage of the disease.[114] Some studies show that the loss of neocortical synapses in subjects with AD correlates strongly with an increase in the numbers of plaques,[118] whereas other studies show the lack of correlation between synaptic density and senile plaques.[113,116,117] These discrepant results are likely to be related to whether synaptic markers were evaluated in the neocortical neuropil that contained or was free of senile plaques. In the present study, we show by EM that morphological changes at synapses are associated with senile plaque formation. Many ultrastructural changes that occur at synapses in the early stages of senile plaque formation resemble patterns of anterograde, retrograde, and transsynaptic degeneration in experimental lesion studies.[119–122] In the cerebral cortex of aged monkey, the intracellular accumulation of APP and nonfibrillar Aβ within neurites and glia may be a response of some cellular populations to the disruption of normal afferent-target integrity that results from the degeneration of afferent nerve terminals and postsynaptic dendritic targets. In this concept, the intracellular formation of Aβ within denervated dendrites and reactive glia (Figure 14) would result from up-regulation of APP and abnormal processing of APP to amyloidogenic derivatives through the endosomal-lysosomal system.[26,27] As neurons and their dendrites degenerate and as activated glia and their processes turn over (expand and retract), Aβ could be released into the extracellular compartment, and/or released amyloidogenic derivatives could serve as substrates for proteases (α_1-antichymotrypsin) found within glia that have infiltrated into the foci of injury. Our findings that Aβ immunoreactivity is localized within neuronal lysosomes/lipofuscin granules and that Aβ is produced by reactive astrocytes and microglia are consistent with this hypothesis, and our inability to detect APP immunoreactivity within lysosomes may reflect the absence of APP within these organelles, the lack of accumulation of APP in lysosomes in amounts that are immunologically detectable, or rapid processing of APP into nonantigenic derivatives. Additional support for this concept is found in data showing that the deafferentation of neocortex causes an increased expression of APP within cerebral cortex[123] and that lesions in the hippocampus induce an increase in APP immunoreactivity within astrocytes in the vicinity of neuronal damage.[36] Moreover, as suggested by *in vitro* studies of the neurotoxicity of Aβ,[124,125] it is possible that the chronic deposition of extracellular amyloid fibrils within the brain parenchyma may further potentiate synaptic disjunction and glial activation in the aged cerebral cortex. We believe that synaptic pathology, possibly resulting from aberrations in cell adhesion or extracellular matrix molecules, and glial responses to synaptic injury may be causal mechanisms that underlie the spontaneous development of senile plaques and deposits of amyloid within the aging cerebral cortex.

Acknowledgments

The authors thank Ms. Judith Van Lare for her expert technical assistance. We also thank Drs. Konrad Beyreuther, Colin Masters, Tilman Olsterdorf, and Edward Koo for generously providing antibodies to Aβ or APP, as well as Dr. Barbara Hansen (Washington Regional Primate Center) and the Baltimore Zoological Society for their cooperation.

References

1. Redlich E: Ueber miliare Sklerose der Hirnrinde bei seniler Atrophie. Jahrb Psychiatr Neurol 1898, 17: 208–216
2. Alzheimer A: Über eine eigenartige Erkrankung der Hirnrinde. Allg Z Psychiatrie Psychisch-Gerichlich Med 1907, 64:146–148
3. Simchowicz VT: Histologische Studien über die senile Demenz. Histologische und Histopathologische Arbeiten über die Grosshirnrinde mit Besonderer Berucksichtigung der Pathologischen Anatomie der Geisteskrankheiten. Edited by F Nissl and A Alzheimer. Jena, Germany, Gustav Fischer Verlag, 1911, pp 267–444
4. Ferraro A: The origin and formation of senile plaques. Arch Neurol Psychiatry 1931, 25:1042–1062
5. Soniat TLL: Histogenesis of senile plaques. Arch Neurol Psychiatry 1941, 46:101–114
6. Liss L: Senile brain changes. Histopathology of the ganglion cells. J Neuropathol Exp Neurol 1960, 19: 559–571
7. Kidd M: Alzheimer's disease: an electron microscopical study. Brain 1964, 87:307–320
8. Luse SA, Smith KR Jr. The ultrastructure of senile plaques. Am J Pathol 1964, 44:553–563
9. Terry RD, Gonatas NK, Weiss M: Ultrastructural studies in Alzheimer's presenile dementia. Am J Pathol 1964, 44:269–297
10. Wisniewski HM, Terry RD: Reexamination of the pathogeneisis of the senile plaque. Progress in Neuropathology. Edited by HM Zimmerman. New York, Grune and Stratton, 1973, pp 1–26
11. Allsop D, Landon M, Kidd M: The isolation and amino acid composition of senile plaque core protein. Brain Res 1983, 259:348–352
12. Masters CL, Simms G, Weinman NA, Multhaup G, McDonald BL, Beyreuther K: Amyloid plaque core protein in Alzheimer disease and Down syndrome. Proc Natl Acad Sci USA 1985, 82:4245–4249
13. Wong CW, Quaranta V, Glenner GG: Neuritic plaques and cerebrovascular amyloid in Alzheimer disease are antigenically related. Proc Natl Acad Sci USA 1985, 82:8729–8732
14. Müller-Hill B, Beyreuther K: Molecular biology of Alzheimer's disease. Annu Rev Biochem 1989, 58:287–307
15. Kang J, Lemaire H-G, Unterbeck A, Salbaum JM, Masters CL, Grzeschik K-H, Multhaup G, Beyreuther K, Müller-Hill B: The precursor of Alzheimer's disease amyloid A4 protein resembles a cell-surface receptor. Nature 1987, 325:733–736
16. Dyrks T, Weidemann A, Multhaup G, Salbaum JM, Lemaire H-G, Kang J, Müller-Hill B, Masters CL, Beyreuther K: Identification transmembrane orientation biogenesis of the amyloid A4 precursor of Alzheimer's disease. EMBO J 1988, 7:949–957
17. Weidemann A, König G, Bunke D, Fischer P, Salbaum JM, Masters CL, Beyreuther K: Identification biogenesis localization of precursors of Alzheimer's disease A4 amyloid protein. Cell 1989, 57:115–126
18. Goldgaber D, Lerman MI, McBride OW, Saffiotti U, Gajdusek DC: Characterization and chromosomal localization of a cDNA encoding brain amyloid of Alzheimer's disease. Science 1987, 235:877–880
19. Tanzi RE, Gusella JF, Watkins PC, Bruns GAP, St. George-Hyslop P, Van Keuren ML, Patterson D, Pagan S, Kurnit DM, Neve RL: Amyloid β protein gene: cDNA, mRNA distribution, and genetic linkage near the Alzheimer locus. Science 1987, 235:880–884
20. Kitaguchi N, Takahashi Y, Tokushima Y, Shiojiri S, Ito H: Novel precursor of Alzheimer's disease amyloid protein shows protease inhibitory activity. Nature 1988, 331:530–532
21. Schubert D, Schroeder R, LaCorbiere M, Saitoh T, Cole G: Amyloid β protein precursor is possibly a heparan sulfate proteoglycan core protein. Science 1988, 241:223–226
22. Esch FS, Keim PS, Beattie EC, Blacher RW, Culwell AR, Oltersdorf T, McClure D, Ward PJ: Cleavage of amyloid β peptide during constitutive processing of its precursor. Science 1990, 248:1122–1124
23. Sisodia SS, Koo EH, Beyreuther K, Unterbeck A, Price DL: Evidence that β-amyloid protein in Alzheimer's disease is not derived by normal processing. Science 1990, 248:492–495
24. Wang R, Meschia JF, Cotter RJ, Sisodia SS: Secretion of the β/A4 amyloid precursor protein. Identification of a cleavage site in cultured mammalian cells. J Biol Chem 1991, 266:16960–16964
25. Sisodia SS: β-amyloid precursor protein cleavage by a membrane-bound protease. Proc Natl Acad Sci USA 1992, 89:6075–6079
26. Cole GM, Huynh TV, Saitoh T: Evidence for lysosomal processing of amyloid β-protein precursor in cultured cells. Neurochem Res 1989, 14:933–939
27. Golde TE, Estus S, Younkin LH, Selkoe DJ, Younkin SG: Processing of the amyloid protein precursor to potentially amyloidogenic derivatives. Science 1992, 255:728–730
28. Haass C, Schlossmacher MG, Hung AY, Vigo-Pelfrey C, Mellon A, Ostaszewski BL, Lieberburg I, Koo EH, Schenk D, Teplow DB, Selkoe DJ: Amyloid β-peptide is produced by cultured cells during normal metabolism. Nature 1992, 359:322–325
29. Seubert P, Vigo-Pelfrey C, Esch F, Lee M, Dovey H, Davis D, Sinha S, Schlossmacher M, Whaley J, Swindlehurst C, McCormack R, Wolfert R, Selkoe D, Lieberburg I, Schenk D: Isolation and quantification of soluble Alzheimer's β-peptide from biological fluids. Nature 1992, 359:325–327
30. Shoji M, Golde TE, Ghiso J, Cheung TT, Estus S, Shaffer LM, Cai X-D, McKay DM, Tintner R, Frangione B, Younkin SG: Production of the Aizheimer amyloid β protein by normal proteolytic processing.

Science 1992, 258:126–129
31. Chartier-Harlin M-C, Crawford F, Houlden H, Warren A, Hughes D, Fidani L, Goate A, Rossor M, Roques P, Hardy J, Mullan M: Early-onset Alzheimer's disease caused by mutations at codon 717 of the β-amyloid precursor protein gene. Nature 1991, 353: 844–846
32. Goate A, Chartier-Harlin M-C, Mullan M, Brown J, Crawford F, Fidani L, Giuffra L, Haynes A, Irving N, James L, Mant R, Newton P, Rooke K, Roques P, Talbot C, Pericak-Vance M, Roses A, Williamson R, Rossor M, Owen M, Hardy J: Segregation of a missense mutation in the amyloid precursor protein gene with familial Alzheimer's disease. Nature 1991, 349:704–706
33. Naruse S, Igarashi S, Kobayashi H, Aoki K, Inuzuka T, Kaneko K, Shimizu T, Iihara K, Kojima T, Miyatake T, Tsuji S: Mis-sense mutation Val → Ile in exon17 of amyloid precursor protein gene in Japanese familial Alzheimer's disease. Lancet 1991, 337:978–979
34. Schubert D: The possible role of adhesion in synaptic modification. Trends Neurosci 1991, 14:127–130
35. Masters CL, Multhaup G, Simms G, Pottgiesser J, Martins RN, Beyreuther K: Neuronal origin of a cerebral amyloid: neurofibrillary tangles of Alzheimer's disease contain the same protein as the amyloid of plaque cores and blood vessels. EMBO J 1985, 4:2757–2763
36. Siman R, Card JP, Nelson RB, Davis LG: Expression of β-amyloid precursor protein in reactive astrocytes following neuronal damage. Neuron 1989, 3:275–285
37. Wisniewski HM, Wegiel J, Wang KC, Kujawa M, Lach B: Ultrastructural studies of the cells forming amyloid fibers in classical plaques. Can J Neurol Sci 1989, 16:535–542
38. Cataldo AM, Nixon RA: Enzymatically active lysosomal proteases are associated with amyloid deposits in Alzheimer brain. Proc Natl Acad Sci USA 1990, 87: 3861–3865
39. Cork LC, Masters C, Beyreuther K, Price DL: Development of senile plaques. Relationships of neuronal abnormalities and amyloid deposits. Am J Pathol 1990, 137:1383–1392
40. Martin LJ, Sisodia SS, Koo EH, Cork LC, Dellovade TL, Weidemann A, Beyreuther K, Masters C, Price DL: Amyloid precursor protein in aged nonhuman primates. Proc Natl Acad Sci USA 1991, 88:1461–1465
41. Peters A: Aging in monkey cerebral cortex. Normal and Altered States of Function: Cerebral Cortex. Edited by A Peters and EG Jones. New York, Plenum Press, 1991, pp 485–510
42. Podlisny MB, Tolan DR, Selkoe DJ: Homology of the amyloid β protein precursor in monkey and human supports a primate model for β amyloidosis in Alzheimer's disease. Am J Pathol 1991, 138:1423–1435
43. Selkoe DJ: The molecular pathology of Alzheimer's disease. Neuron 1991, 6:487–498
44. Wong-Riley M: Changes in the visual system of monocularly sutured or enucleated cats demonstrable with cytochrome oxidase histochemistry. Brain Res 1979, 171:11–28
45. Vincent SR, Johansson O, Hökfelt T, Skirboll L, Elde RP, Terenius L, Kimmel J, Goldstein M: NADPH-diaphorase: a selective histochemical marker for striatal neurons containing both somatostatin- and avian pancreatic polypeptide (APP)-like immunoreactivities. J Comp Neurol 1983, 217:252–263
46. Oltersdorf T, Ward PJ, Henriksson T, Beattie EC, Neve R, Lieberburg I, Fritz LC: The Alzheimer amyloid precursor protein. Identification of a stable intermediate in the biosynthetic/degradative pathway. J Biol Chem 1990, 265:4492–4497
47. Levey AI, Bolam JP, Rye DB, Hallanger AE, Demuth RM, Mesulam M-M, Wainer BH: A light and electron microscopic procedure for sequential double antigen localization using diaminobenzidine and benzidine dihydrochloride. J Histochem Cytochem 1986, 34: 1449–1457
48. Martin LJ, Blackstone CD, Levey AI, Huganir RL, Price DL: Cellular localizations of AMPA glutamate receptors within the basal forebrain magnocellular complex of rat and monkey. J Neurosci 1993, 13: 2249–2263
49. Shivers BD, Hilbich C, Multhaup G, Salbaum M, Beyreuther K, Seeburg PH: Alzheimer's disease amyloidogenic glycoprotein: expression pattern in rat brain suggests a role in cell contact. EMBO J 1988, 7:1365–1370
50. Bahmanyar S, Higgins GA, Goldgaber D, Lewis DA, Morrison JH, Wilson MC, Shankar SK, Gajdusek DC: Localization of amyloid β protein messenger RNA in brains from patients with Alzheimer's disease. Science 1987, 237:77–79
51. Koo EH, Sisodia SS, Cork LC, Unterbeck A, Bayney RM, Price DL: Differential expression of amyloid precursor protein mRNAs in case of Alzheimer's disease and in aged nonhuman primates. Neuron 1990, 2:97–104
52. Neve RL, Finch EA, Dawes LR: Expression of the Alzheimer amyloid precursor gene transcripts in the human brain. Neuron 1988, 1:669–677
53. Card JP, Meade RP, Davis LG: Immunocytochemical localization of the precursor protein for β-amyloid in the rat central nervous system. Neuron 1988, 1:835–846
54. Benowitz LI, Rodriguez W, Paskevich P, Mufson EJ, Schenk D, Neve RL: The amyloid precursor protein is concentrated in neuronal lysosomes in normal and Alzheimer disease subjects. Exp Neurol 1989, 106: 237–250
55. Tate-Ostroff B, Majocha RE, Marotta CA: Identification of cellular and extracellular sites of amyloid precursor protein extracytoplasmic domain in normal

and Alzheimer disease brains. Proc Natl Acad Sci USA 1989, 86:745–749
56. Kawarabayashi T, Shoji M, Harigaya Y, Yamaguchi H, Hirai S: Expression of APP in the early stage of brain damage. Brain Res 1991, 563:334–338
57. Coria F, Moreno A, Torres A, Ahmad I, Ghiso J: Distribution of Alzheimer's disease amyloid protein precursor in normal human and rat nervous system. Neuropathol Appl Neurobiol 1992, 18:27–35
58. McGeer PL, Akiyama H, Kawamata T, Yamada T, Walker DG, Ishii T: Immunohistochemical localization of β-amyloid precursor protein sequences in Alzheimer and normal brain tissue by light and electron microscopy. J Neurosci Res 1992, 31:428–442
59. Schubert W, Prior R, Weidemann A, Dircksen H, Multhaup G, Masters CL, Beyreuther K: Localization of Alzheimer βA4 amyloid precursor protein at central and peripheral synaptic sites. Brain Res 1991, 563: 184–194
60. Shigematsu K, McGeer PL, McGeer EG: Localization of amyloid precursor protein in selective postsynaptic densities of rat cortical neurons. Brain Res 1992, 593:353–357
61. Shoji M, Hirai S, Yamaguchi H, Harigaya Y, Kawarabayashi T: Amyloid β-protein precursor accumulates in dystrophic neurites of senile plaques in Alzheimer-type dementia. Brain Res 1990, 512:164–168
62. Joachim C, Games D, Morris J, Ward P, Frenkel D, Selkoe D: Antibodies to non-β regions of the β-amyloid precursor protein detect a subset of senile plaques. Am J Pathol 1991, 138:373–384
63. Haass C, Hung AY, Selkoe DJ: Processing of β-amyloid precursor protein in microglia and astrocytes favors an internal localization over constitutive secretion. J Neurosci 1991, 11:3783–3793
64. Yamaguchi H, Yamazaki T, Ishiguro K, Shoji M, Nakazato Y, Hirai S: Ultrastructural localization of Alzheimer amyloid β/A4 protein precursor in the cytoplasm of neurons and senile plaque-associated astrocytes. Acta Neuropathol 1992, 85:15–22
65. Goldgaber D, Harris HW, Hla T, Maciag T, Donnelly RJ, Jacobsen JS, Vitek MP, Gajdusek DC: Interleukin 1 regulates synthesis of amyloid-protein precursor mRNA in human endothelial cells. Proc Natl Acad Sci USA 1989, 86:7606–7610
66. Yamazaki T, Yamaguchi H, Kawarabayashi T, Hirai S: Ultrastructural localization of amyloid β/A4 protein precursor in the normal rat brain. Virchows Arch B Cell Pathol 1993, 63:173–180
67. Schubert D, Jin L-W, Saitoh T, Cole G: The regulation of amyloid β protein precursor secretion and its modulatory role in cell adhesion. Neuron 1989, 3:689–694
68. Kametani F, Haga S, Tanaka K, Ishii T: Amyloid B-protein (APP) of cultured cells: secretory and nonsecretory forms of APP. J Neurol Sci 1990, 97:43–52
69. Klier FG, Cole G, Stalleup W, Schubert D: Amyloid β-protein precursor is associated with extracellular matrix. Brain Res 1990, 515:336–342
70. Octave J-N de Sauvage F, Maloteaux J-M: Modification of neuronal cell adhesion affects the genetic expression of the A4 amyloid peptide precursor. Brain Res 1989, 486:369–371
71. Breen KC, Bruce M, Anderton BH: Beta amyloid precursor protein mediates neuronal cell-cell and cell-surface adhesion. J Neurosci Res 1991, 28:90–100
72. Chen M, Yankner BA: An antibody to β amyloid and the amyloid precursor protein inhibits cell-substratum adhesion in many mammalian cell types. Neurosci Lett 1991, 125:223–226
73. Saitoh T, Sundsmo M, Roch J-M, Kimura T, Cole G, Schubert D, Oltersdorf T, Schenk DB: Secreted form of amyloid β protein precursor is involved in the growth regulation of fibroblasts. Cell 1989, 58:615–622
74. Masliah E, Mallory M, Ge N, Saitoh T: Amyloid precursor protein is localized in growing neurites of neonatal rat brain. Brain Res 1992, 593:323–328
75. Milward EA, Papadopoulos R, Fuller SJ, Moir RD, Small D, Beyreuther K, Masters CL: The amyloid protein precursor of Alzheimer's disease is a mediator of the effects of nerve growth factor on neurite outgrowth. Neuron 1992, 9:129–137
76. Fisher S, Gearhart JD, Oster-Granite ML: Expression of the amyloid precursor protein gene in mouse oocytes and embryos. Proc Natl Acad Sci USA 1991, 88:1779–1782
77. Shigematsu K, McGeer PL, Walker DG, Ishii T, McGeer EG: Reactive microglia/macrophages phagocytose amyloid precursor protein produced by neurons following neural damage. J Neurosci Res 1992, 31: 443–453
78. Habener JF: Principles of peptide-hormone biosynthesis. Neurosecretion and Brain Peptides. Edited by JB Martin, S Reichlin, and KL Bick. New York, Raven Press, 1981, pp 21–34
79. Xie C-W, Mitchell CL, Hong J-S: Perforant path stimulation differentially alters prodynorphin mRNA and proenkephalin mRNA levels in the entorhinal cortex-hippocampal region. Mol Brain Res 1990, 7:199–205
80. Zafra F, Hengerer B, Leibrock J, Thoenen H, Lindholm D: Activity dependent regulation of BDNF and NGF mRNAs in the rat hippocampus is mediated by non-NMDA glutamate receptors. EMBO J 1990, 9:3545–3550
81. Sun Y, Rao MS, Landis SC, Zigmond RE: Depolarization increases vasoactive intestinal peptide- and substance P-like immunoreactivities in cultured neonatal and adult sympathetic neurons. J Neurosci 1992, 12: 3717–3728
82. Lahiri DK, Robakis NK: The promoter activity of the gene encoding Alzheimer β-amyloid precursor protein (APP) is regulated by two blocks of upstream sequences. Mol Brain Res 1991, 9:253–257

83. Dickson DW, Crystal HA, Mattiace LA, Masur DM, Blau AD, Davies P, Yen S-H, Aronson MK: Identification of normal and pathological aging in prospectively studied nondemented elderly humans. Neurobiol Aging 1991, 13:179–189
84. Delaére P, He Y, Fayet G, Duyckaerts C, Hauw J-J: βA4 deposits are constant in the brain of the oldest old: an immunocytochemical study of 20 French centenarians. Neurobiol Aging 1993, 14:191–194
85. Kawas C, Martin LJ, Troncoso JC: Paucity of senile plaques and neurofibrillary tangles in neocortex of nondemented individuals. Neurology 1992, 42(Suppl. 3):444
86. Troncoso JC, Martin LJ, Gorman LK, Kawas CH: Morphological and neurochemical observations on the neocortices of elderly nondemented individuals. J Neuropathol Exp Neurol 1992, 51:326
87. Hyman BT, Van Hoesen GW, Damasio AR: Memory-related neural systems in Alzheimer's disease: an anatomic study. Neurology 1990, 40:1721–1730
88. Wisniewski HM, Ghetti B, Terry RD: Neuritic (senile) plaques filamentous changes in aged rhesus monkeys. J Neuropathol Exp Neurol 1973, 32:566–584
89. Yamaguchi H, Nakazato Y, Hirai S, Shoji M, Harigaya Y: Electron micrograph of diffuse plaques. Initial stage of senile plaque formation in the Alzheimer brain. Am J Pathol 1989, 135:593–597
90. Yamaguchi H, Nakazato Y, Hirai S, Shoji M: Immunoelectron microscopic localization of amyloid β protein in the diffuse plaques of Alzheimer-type dementia. Brain Res 1990, 508:320–324
91. Gonatas NK, Anderson W, Evangelista I: The contribution of altered synapses in the senile plaque: an electron microscopic study in Alzheimer's dementia. J Neuropathol Exp Neurol 1967, 26:25–39
92. Miyakawa T, Shimoji A, Kuramoto R, Higuchi Y: The relationship between senile plaques and cerebral blood vessels in Alzheimer's disease and senile dementia. Morphological mechanism of senile plaque production. Virchows Arch B Cell Pathol 1982, 40: 121–129
93. Allsop D, Haga S-I, Haga C, Ikeda S-I, Mann DMA, Ishii T: Early senile plaques in Down's syndrome brains show a close relationship with cell bodies of neurons. Neuropathol Appl Neurobiol 1989, 15:531–542
94. Probst A, Langui D, Ipsen S, Robakis N, Ulrich J: Deposition of β/A4 protein along neuronal plasma membranes in diffuse senile plaques. Acta Neuropathol 1991, 83:21–29
95. Frackowiak J, Wisniewski HM, Wegiel J, Merz GS, Iqbal K, Wang KC: Ultrastructure of the microglia that phagocytose amyloid and the microglia that produce β-amyloid fibrils. Acta Neuropathol 1992, 84:225–233
96. Yamaguchi H, Nakazato Y, Shoji M, Takatama M, Hirai S: Ultrastructure of diffuse plaques in senile dementia of the Alzheimer type: comparison with primitive plaques. Acta Neuropathol 1991, 82:13–20
97. Roher A, Gray EG, Paula-Barbosa M: Alzheimer's disease: coated vesicles, coated pits and the amyloid-related cell. Proc R Soc Lond Ser B Biol Sci 1988, 232:367–373
98. Perry G, Lipphardt S, Kancherla M, Gambetti P, Maggiora L, Lobl T, Mulvihill P, Mijares M, Sharma S, Cornette J, Greenberg B: Amyloid precursor protein in senile plaques of Alzheimer's disease. Lancet 1988, 2:746
99. Ishii T, Kametani F, Haga S, Sato M: The immunohistochemical demonstration of subsequences of the precursor of the amyloid A4 protein in senile plaques in Alzheimer's disease. Neuropathol Appl Neurobiol 1989, 15:135–147
100. Cras P, Kawai M, Lowery D, Gonzalez-DeWhitt P, Greenberg B, Perry G: Senile plaque neurites in Alzheimer disease accumulate amyloid precursor protein. Proc Natl Acad Sci USA 1991, 88:7552–7556
101. Cummings BJ, Su JH, Geddes JW, Van Nostrand WE, Wagner SL, Cunningham DD, Cotman CW: Aggregation of the amyloid precursor protein within degenerating neurons and dystrophic neurites in Alzheimer's disease. Neuroscience 1992, 48:763–777
102. Koo EH, Sisodia SS, Archer DR, Martin LJ, Weidemann A, Beyreuther K, Fischer P, Masters CL, Price DL: Precursor of amyloid protein in Alzheimer disease undergoes fast anterograde axonal transport. Proc Natl Acad Sci USA 1990, 87:1561–1565
103. Sisodia SS, Koo EH, Hoffman PN, Perry G, Price DL: Identification and transport of full-length amyloid precursor proteins in rat peripheral nervous system. J Neurosci 1993, 13:3136–3142
104. Scott JN, Parhad IM, Clark AW: β-amyloid precursor protein gene is differentially expressed in axotomized sensory and motor systems. Mol Brain Res 1991, 10: 315–325
105. Streit WJ: Microglial-neuronal interactions. J Chem Neuroanat 1993, 6:261–266
106. Johnson SA, Lampert-Etchells M, Pasinetti GM, Rozovsky I, Finch CE: Complement mRNA in the mammalian brain: responses to Alzheimer's disease and experimental brain lesioning. Neurobiol Aging 1992, 13:641–648
107. Siman R, Card JP, Davis LG: Proteolytic processing of β-amyloid precursor by calpain I. J Neurosci 1990, 10:2400–2411
108. Razzaboni RL, Papastoitsis G, Koo EH, Abraham CR: A calcium- stimulated serine protease from monkey brain degrades the β-amyloid precursor protein. Brain Res 1992, 589:207–216
109. Dawson TM, Dawson VL, Snyder SH: A novel neuronal messenger molecule in brain: the free radical, nitric oxide. Ann Neurol 1994, 32:297–311
110. Takashima S, Kuruta H, Mito T, Nishizawa M, Kunishita T, Tabira T: Developmental and aging changes in the expression patterns of β-amyloid in the brains of normal and Down syndrome cases. Brain Dev 1990, 12:367–371

111. Adams I: Plasticity of the synaptic contact zone following loss of synapses in the cerebral cortex of aging humans. Brain Res 1987, 424:343–351
112. Adams I: Comparison of synaptic changes in the precentral and postcentral cerebral cortex of aging humans: a quantitative ultrastructural study. Neurobiol Aging 1987, 8:203–212
113. Masliah E, Mallory M, Hansen L, DeTeresa R, Terry RD: Quantitative synaptic alterations in the human neocortex during normal aging. Neurology 1993, 43: 192–197
114. Davies CA, Mann DMA, Sumpter PQ, Yates PO: A quantitative morphometric analysis of the neuronal and synaptic content of the frontal and temporal cortex in patients with Alzheimer's disease. J Neurol Sci 1987, 78:151–164
115. Hamos JE, DeGennaro LJ, Drachman DA: Synaptic loss in Alzheimer's disease and other dementias. Neurology 1989, 39:355–361
116. Masliah E, Terry RD, DeTeresa RM, Hansen LA: Immunohistochemical quantification of the synapse-related protein synaptophysin in Alzheimer disease. Neurosci Lett 1989, 103:234–239
117. Scheff SW, DeKosky ST, Price DA: Quantitative assessment of cortical synaptic density in Alzheimer's disease. Neurobiol Aging 1990, 11:29–37
118. Adams IM: Structural plasticity of synapses in Alzheimer's disease. Mol Neurobiol 1992, 5:411–419
119. Gray EG: The fine structure of normal degenerating synapses of the central nervous system. Arch Biol (Liège) 1964, 75:285–299
120. Kawana E, Akert K, Bruppacher H: Enlargement of synaptic vesicles as an early sign of terminal degeneration in the rat caudate nucleus. J Comp Neurol 1971, 142:297–308
121. Hattori T, Fibiger HC: On the use of lesions of afferents to localize neurotransmitter receptor sites in the striatum. Brain Res 1982, 238:245–250
122. Pearson HE, Stoffler DJ, Sonstein WJ: Response of retinal terminals to loss of postsynaptic target neurons in the dorsal lateral geniculate nucleus of the adult cat. J Comp Neurol 1992, 315:333–343
123. Wallace WC, Bragin V, Robakis NK, Sambamurti K, VanderPutten D, Merril CR, Davis KL, Santucci AC, Haroutunian V: Increased biosynthesis of Alzheimer amyloid precursor protein in the cerebral cortex of rats with lesions of the nucleus basalis of Meynert. Mol Brain Res 1991, 10:173–178
124. Yankner BA, Dawes LR, Fisher S, Villa-Komaroff L, Oster-Granite ML, Neve RL: Neurotoxicity of a fragment of the amyloid precursor associated with Alzheimer's disease. Science 1989, 245:417–420
125. Pike CJ, Walencewicz AJ, Glabe CG, Cotman CW: In vitro aging of β-amyloid protein causes peptide aggregation neurotoxicity. Brain Res 1991, 563:311–314